NTNU – Trondheim
Norwegian University of
Science and Technology

EFFECTIVE ANISOTROPY VERSUS FLUID SATURATION

Chone Lugangizya Malembo

Petroleum Geosciences
Submission date: August 2015
Supervisor: Alexey Stovas, IPT

Norwegian University of Science and Technology
Department of Petroleum Engineering and Applied Geophysics

NTNU Norwegian University of Science and Technology
Faculty of Engineering Science and Technology
Department of Petroleum Engineering and Applied Geophysics.

Effective anisotropy from thinly layered reservoir versus fluid saturation

A thesis by

MALEMBO, Chone Lugangizya.

Submitted at the Norwegian University of Science and Technology, Department of Petroleum Engineering and Applied Geophysics in partial fulfilment of the requirements for award of a masters degree in Petroleum Geophysics.

Submitted: Tuesday, August 11, 2015

Preface

I am indebted to express my heartfelt gratitude to the almighty God for keeping me healthier during the whole time when working on this thesis.

Many thanks go to my lovely wife Mrs. Gaudensia Nyamate for being patient and for her encouragement throughout this time.

I also, am indebted to express my heartfelt gratitude to Prof. Alexey Stovas for his support, assistance and guidance without which this work would have not been successful.

I am very grateful for Dr. Isaac Marobhe of the Department of Geology, University of Dar es salaam for his supervision, revision, guidance and proof reading this work.

The last but not least of my thanks go to the ANTHEI group of students for their assistances at different stages that have all made this work a reality.

Dedication

This work is dedicated to my newly born baby boy, Malembo.

Abstract

Anisotropy has proved to be a reliable means for determination of the rock properties necessary to characterize the subsurface. VTI is a form of anisotropy which provides an estimate of the layered earth.

This report summarises a work done on well data acquired in one well in Cote d'Ivore. The data consisted P- and S-waves velocities and density of isotropic thin layers at different fluid saturations.

Backus averaging was used for creation of the effective medium in the form VTI. Stiffness coefficients of the effective media were then determined from which the vertical P- and S-waves velocities were calculated.

Additionally, the three anisotropy parameters, epsilon, delta and gamma were calculated for each fluid saturation.

Analysis of the variation of all the five parameters has been made, from which the P-wave velocity has been found to increase when water is in the pores as compared to oil and gas. Fluid substitution has been found to have a negligible effect on S-wave velocity and gamma.

Gas has also been found to have the largest effect on P-wave anisotropy. The moveout parameter delta has been observed to have a more complex response to fluid substitution bringing an attention and a call to revisiting the conclusion that eta is invariant of fluid saturation.

Contents

Preface....i

Dedication....ii

Abstract....iii

Contents....iv

Table of figures....v

1. Introduction....1

1.1. General introduction....1

1.2. Research objectives....3

1.3. Available data....6

1.4. Research methodology and workflow....7

1.5. Significance of the study....8

1.6. Scope of the study....9

2. Literature review....10

2.1. Elastic anisotropy....10

2.2. Transverse Isotropy with Vertical axis of symmetry, VTI material....13

2.3. Seismic upscaling and the Backus averaging....14

2.4. Fluid substitution....18

3. Results....22

4. Discussion....27

5. Conclusion....31

6. Recommendations....32

7. References 33

8. Appendices 36

Table of figures

Figure 1: Causes of anisotropy in most sedimentary rocks 2

Figure 2: HTI model from vertical cracks 12

Figure 3: A simplified VTI model 12

Figure 4: Vp0 at different fluid saturations 23

Figure 5: Vs0 at different fluid saturations 23

Figure 6: gamma at different fluid saturations 24

Figure 7: epsilon at different fluid saturations 25

Figure 8: delta at different fluid saturations 26

1. Introduction

1.1. General introduction

It is well recognized that sedimentary rocks are not, in general, elastically isotropic, but suffer from some degree of anisotropy (Norris and Sinha, 1993). Despite this fact**, i**n common exploration geophysics rocks in the subsurface are assumed to be isotropic. This common treatment stems from the fact that anisotropic wave equations are complex and therefore hard to grasp intuitively. The scope of measurements whereby only few parameters are obtainable in most experiments, which cannot fully characterize an anisotropic elastic tensor, brings another problem for assuming anisotropic earth model. Besides, the anisotropic Gassmann's fluid substitution is usually expressed in terms of stiffness or compliance coefficients that do not provide an intuitive understanding of how fluid affects the anisotropy (Collet and Gurevich, 2013). Anisotropy may arise from intrinsic microstructural effects such as layering of thin zones, or from local biaxial or triaxial tectonic stresses within the formation (Norris and Sinha, 1993). Other sources are preferential alignment of grains in a particular direction, variation in grain size, shape and inherent crystal defects in some materials where different crystal arrangements might be present in the same material due to packing. Some causes of intrinsic anisotropy are summarized in (Figure 1).

Recent advances in parameter estimation and seismic processing have allowed incorporation of anisotropic models into a wide range of seismic methods (Tsvankin et al. 2010). There also have been several advances in simplification of the anisotropic earth model. Simplifications of the wave equation based on anisotropy is made possible by assuming different shapes and therefore different symmetries as perceived to how the waves sees the subsurface when propagating through it.

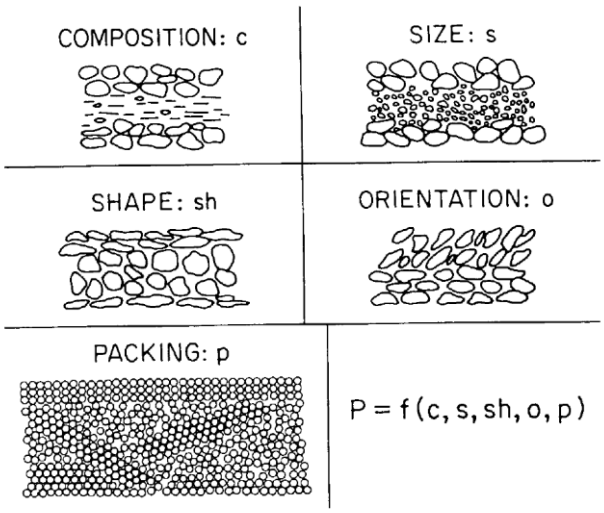

Figure 1: Causes of anisotropy in most sedimentary rocks

(Ruger, 1998) gives examples of the different symmetries as may be experienced by waves traversing the subsurface. A system of parallel penny-shaped vertical cracks embedded in an isotropic matrix gives a Transverse Isotropy with Horizontal axis of symmetry (HTI), a system of two orthogonal but not necessarily identical crack systems or two identical crack systems at oblique angle lead to orthorhombic symmetry also horizontally layered earth with vertical cracks leads to orthorhombic medium (Ruger, 1998). A material which is generally horizontally layered or horizontally fractured with no vertical cracks is considered Transverse Isotropy with a vertical axis of symmetry (VTI). Thin isotropic elastic layering in the earth is one cause of seismic VTI anisotropy, along with intrinsic anisotropy and fractures (Liner and Fei, 2006). The VTI medium is one of the commonest medium used in the study of the behaviour of the layered earth and which has proved to provide a reasonable estimation to different parameters characterizing the properties of rocks in the subsurface.

While rocks in the subsurface are anisotropic, atleast weakly anisotropic, the general and simplest isotropic assumptions does not provide an accurate estimate of the properties of rocks in the subsurface. One of the basic assumptions to simplifying the wave equation for waves propagating in a layered earth model is regarding the material as being Transverse

Isotropy (TI). A transverse isotropy material has two orthogonal directions in which the material exhibits similar properties. Assuming horizontally stratified earth model, the earth will therefore be a Transverse Isotropy with the Vertical axis of symmetry (VTI). This means waves propagating vertically (along Z-directions) will have similar properties in the orthogonally two horizontal directions (X and Y directions).

1.2. **Research objectives**

The importances of considering anisotropy to estimating the subsurface features and structures have for long time being studied. Hydrocarbon-saturated reservoirs have shown significant complexity in both their lithology and corresponding seismic response (Li, 2013)**.** Use of isotropic approximation based on Gassmann (1951) equations have been shown by (Mavko and Bandyopadhyay, 2009) to over predict the anisotropic results and to under predict the same in some other cases. This brings an attention to considering anisotropic approximations instead of their isotropic equivalences. Anisotropy is usually expressed in terms of the three anisotropic parameters epson (ε), delta (δ) and gamma (γ) with determination of the vertical P- and S-waves velocities (these parameters are defined in equation (12)). The parameter ε is close to the fractional difference between the P-wave velocities in the directions perpendicular and parallel to the symmetry axis, so it defines what is often simplistically called the "P-wave anisotropy (Tsvankin et al., 2010) and (Thomsen, 1986) refers to this as the anisotropy of the rock. (Thomsen, Weak elastic anisotropy, 1986) has shown that the contribution from the parameter ε dominates the seismic anisotropy in near horizontal seismic wave's propagations. On the other hand, the parameter, δ (Delta) which controls the near-vertical anisotropy is a different combination of elastic moduli, which does not include C_{11} (i.e., the horizontal velocity) at all (Thomsen, 1986). Thomsen parameter, δ describes near-offset quasi-P-wave NMO (Mavko and Bandyopadhyay, 2009) and it governs the P-wave velocity variation away from the symmetry axis and also

influences the SV-wave velocity (Tsvankin et al., 2010) while Gamma (γ) is the shear wave splitting.

All the three anisotropy parameters with the vertical wave velocities are very important in seismic exploration. Knowledge of ε, vertical P-wave velocity and δ are important in determination of wave velocity at oblique angle. In most exploration geophysics the parameter, δ, is of great importance as it controls near vertical response and most data acquisitions are carried out in this regime. As it is shown in equation (1) as derived in (Thomsen, 1986)for weak anisotropy, δ, γ and vertical velocity are important in determination of moveout velocity required for seismic processing. δ is also important for determination of horizontal stress while the three parameters altogether are very crucial in determining the group velocity and quantification of the degree of anisotropy in a rock.

$$\left\{\begin{array}{c} V_{NMO}(P) = \alpha_0(1+\delta) \\ V_{NMO}(SV) = \beta_0\left[1+\frac{\alpha_0^2}{\beta_0^2}(\varepsilon-\delta)\right] \\ V_{NMO}(SH) = \beta_0(1+\gamma) \\ \frac{\sigma_{11}}{\sigma_{33}} = \frac{C_{11}}{C_{33}} = \left(1-2\frac{\beta_0^2}{\alpha_0^2}\right)+\delta \end{array}\right\} \quad (1)$$

In producing reservoirs, stress field changes as a result of

1. Compaction due to depletion
2. Stretching due to fluid injection in enhancing recovery
3. Pressure buil up due to barriers as a result of small sealing faults

These phenomena inculculate the importance of periodic assessing our reservoirs and making updates into our, processing algorithms and simulation models, of important parameters that are likely to change persuant to changes in stress. Parameters mostly affected by changes in

producing reservoir are coefficient of stiffness and velocity hence changes as well, in anisotropy parameters.

Pore fluids strongly influence the seismic properties of rocks (Batzle and Wang, 1992)
Thomsen (2012) has analyzed the effect of fluid on anisotropy parameters but there has not been an alysis on variation of water saturation with these parameters and a mathematical relationships between them does not exist. Pore fluids form a dynamic system in which both composition and physical phases change with pressure and temperature (Batzle and Wang, 1992). These changes in composition and phases have a consequent effect on the basic fluid properties which influence the properties of the entire rock mass as well. (Collet and Gurevich, 2013) have observed that pore fluids are isotropic and therefore they tend to reduce the overall degree of anisotropy without clearly substantiating which fluid has a large effect and why.

This study is designed to make an anlyisis of the variations of anisotropy parameters with fluid composition in a Transverse Isotropic material with vertical axis of symmetry (VTI). Analyisis between the variation of the three anisotropic parameters with water saturation shall be made and if possible, establishing a mathematical relationship between the parameters. It is also expected that the study will confirm that shear wave splitting parameter does not vary with water saturation (or it does so at a small extent and therefore neglected) as shear waves are independent of fluids. To achieve this objective, three specific objectives have been designed which shall include, in the order stated from the initial to the final stage

1. Backus averaging of thin layers to homogeneous medium
2. Determination of anisotropy parameters
3. Analysis of the variation of anisotropic parameters with fluid saturation

1.3. Available data

In order to achieve the stated objectives, the work requires inputs of individual layer compressional and shear wave velocities (Vp and Vs) and layer density, ρ. This is not the only method for upscaling seismic parameters. Full-wave sonic logs provide a fine layered isotropic elastic model that can be used to calculate anisotropy parameters as a function of depth (Liner and Fei, 2006). Full wave form recordings are not available and therefore the three parameters available will provide a basis for the formation of effective medium by Backus averaging and then calculating stiffness coefficients from which anisotropy parameters and the vertical P- and S-waves velocities will be calculated using Thomsen (1986) equations. The data to be used in this work are derived from a well in the Norwegian North Sea.

Vp, Vs and ρ are provided in four different data files insitu_gas.DAT, insitu_oil.DAT, insitu_wet.DAT and insitu_org.DAT. The first three are data files derived from the Gassmann's fluid substitution corresponding to 80% gas, 80% oil and water fully ssaturated reservoirs respectively while the insitu_org.DAT refers to the original recorded data.

1.4. Research methodology and workflow

With the sole purpose of meeting the objectives stated using the available data through the stated specific objectives, this work shall be accomplished using mathematical programming in Matlab codes. The provided well data in form of Vp, Vs and rho shall be used to calculate stiffness coefficients assuming isotropic material before applying Backus averaging to form an effective medium. Stiffness coefficients of the effective medium so formed shall then be used to calculate the vertical P- and S waves' velocities and the anisotropic parameters.

These tasks shall be accomplished in the following steps

1. Use V_p, V_s and ρ from well data to calculate stiffness parameters assuming isotropy materials for different s_w using equation 2.

$$\left.\begin{array}{c} C_{33j} = \rho_j v_{pj}^2 \\ C_{44j} = \rho_j v_{sj}^2 \\ C_{12j} = C_{33j} - 2C_{44j} \\ C_{13j} = C_{12j} \\ C_{44j} = C_{66j} \end{array}\right\} \qquad (2)$$

2. Upscaling using Backus averaging technique to form an effective medium using stiffness coefficients obtained from step 1 above using equation 13.

3. Calculating the anisotropic parameters using effective medium parameters obtained from step 2 using equation 14.

4. The results from step 3 for each parameter at different fluid saturations shall then be plotted against depth (or block number) and observe the effect of the different fluid saturations on the each effective anisotropy parameter.

The steps 1 to 3 shall be accomplished by programming in Matlab codes while step 4 shall be done either in Matlab codes or in excel. To make the computations easier the data corresponding to each block shall be selected and the code shall be designed to make the

computations for each block performing steps 1 through step 3 presented above. The results for each block shall then be combined in a single excel sheet for plotting purposes.

The Matlab codes used in the computations as per above steps are attached at the end of this report as appendix J.

1.5. Significance of the study

Anisotropy (weak anisotropy) approximations has proved to be a reasonable estimate to the properties of the layered earth as compared to isotropic approximations. (Berryman, James G., 1979) have shown and demonstrated how isotropic assumption has to be rechecked when intending to use shear wave parameters obtained from interpreting compressional wave seismic sections. This observation is important in stressing the usefulness and accuracy with which anisotropic assumptions provide in the parameters under which they have been obtained. Anisotropy is quantified by three anisotropic parameters, Epson (ε), delta (δ) and gamma (γ). The parameters, describing the variation of compressional and shear velocities as a function of polar angle with respect to the symmetry axis, are very useful in quantifying the degree of anisotropy (Collet and Gurevich, 2013). A standard characterization of the effective VTI medium requires an addition of two more parameters the vertical P- and S- waves' velocities making a total of five parameters necessary to characterize an effective VTI medium. The usefulness of all these parameters has been highlighted under the research objective section. One more importance to be highlighted here is based on reservoir monitoring during production stages. Both induced (artificial lift) and natural fluid substitution that occurs in a producing reservoir brings a consequent change in the gross reservoir properties pursuant to changes in bulk modulus as one fluid phase is being replaced by another fluid phase. It is therefore crucial to have an understanding if fluid changes result into changes in the anisotropy parameters or not. This knowledge is important so that our parameters are updated accordingly in case the changes in the gross reservoir properties due

to fluid changes affect anisotropy. This study will therefore cater for this demand so that millions of cash that might be lost due to incorrect parameters in our models are saved. This study will also provide a foundation on which more advanced studies relating fluid saturation and anisotropy parameters are to be conducted.

1.6. Scope of the study

The study is designed to study the variations between fluid saturation and anisotropy parameters Epson, delta and gamma in a layered effective medium assumed to be a Transverse Isotropy with vertical axis of symmetry.

Anisotropy in this case is assumed to only being caused by horizontal layering of sedimentary strata in the subsurface.

This study is therefore, and entirely, devoted to an analysis of fluid saturation variation with anisotropy parameters in a transverse isotropy with vertical axis of symmetry effective medium formed from Backus averaging with fluid substitution based on Gassmann's isotropic fluid substitution assumption.

2. Literature review

2.1. Elastic anisotropy

(Thomsen, 1986) has provided definition of a linearly elastic material as defined by (Nye, 1957) as one in which each component of stress σ_{ij} is linearly dependent upon every component of strain ε_{kl}.

The directional indices may assume values of 1, 2 and 3 corresponding to the three Cartesian coordinates X, Y and Z which brings about nine relations, each involving one component of stress and nine components of strain, mathematically written as

$$\sigma_{ij} = \sum_{k=1}^{3}\sum_{l=1}^{3} C_{ijkl}\varepsilon_{kl}, \quad i,j = 1,2,3. \qquad (3)$$

Where the 3 x 3 x 3 x 3 elastic modulus tensor C_{ijkl} completely characterizes the elasticity of the medium (Thomsen, 1986). In the absence of any symmetry, a material that can be described by a strain-energy function requires 21 independent parameters to completely specify its elastic behaviour (Sayers, 1994). Because of the symmetry of stress ($\sigma_{ij} = \sigma_{ji}$), only six of these equations are independent and because of the symmetry of strain ($\varepsilon_{kl} = \varepsilon_{lk}$) only six of the terms on the right side of each set of equation (3) are independent. Hence, the elasticity may be represented with a change of indices using the Voigt recipe (equation 4)

$$\begin{array}{cccccccccc} ij\ or\ kl: & 11 & 22 & 33 & 32=23 & 31=13 & 21=12 & & \\ \downarrow & \downarrow & \downarrow & \downarrow & \downarrow & \downarrow & \downarrow & \downarrow & & (4) \\ \alpha & \beta & 1 & 2 & 3 & 4 & 5 & 6 & & \end{array}$$

So that the 81 components tensor may be written using a 6 x 6 matrix $C_{\alpha\beta}$.

For isotropic material the matrix is as shown in equation 5

$$C_{\alpha\beta} = \begin{bmatrix} C_{33} & C_{33}-2C_{44} & C_{33}-2C_{44} & 0 & 0 & 0 \\ 0 & C_{33} & C_{33}-2C_{44} & 0 & 0 & 0 \\ 0 & 0 & C_{33} & 0 & 0 & 0 \\ 0 & 0 & 0 & C_{44} & 0 & 0 \\ 0 & 0 & 0 & 0 & C_{44} & 0 \\ 0 & 0 & 0 & 0 & 0 & C_{44} \end{bmatrix} \quad (5)$$

These components are related to the Lame parameters **λ** and **μ** and to the bulk modulus **K** by (Thomsen, 1986)

$C_{33} = \lambda + 2\mu = K + \frac{3}{4}\mu$ and $C_{44} = \mu$ (6)

Presence of different symmetries in different materials brings about different forms of anisotropy. In petroleum seismology, we often encounter two types of anisotropy: transverse isotropy and azimuthal anisotropy (Wang, 2002).

Transverse isotropy also known as hexagonal symmetry, has one unique direction with the other two directions being equivalent. When the vertical axis is the unique direction this material is said to be Transverse Isotropy with a vertical axis of symmetry (VTI) as occurs in horizontally layered sedimentary sequences (Figure 3). It is called Transverse Isotropy with a horizontal axis of symmetry (HTI) when the unique axis is horizontal as is the case in a material with vertical cracks embedded in a homogeneous matrix (Figure 2).

Orthorhombic symmetry encompasses materials which in some cases are a combination of VTI and HTI i.e, a horizontally layered material with a set of vertical cracks falls in the orthorhombic symmetry. Azimuthal anisotropy is caused mainly by stress anisotropy (Wang, 2002).

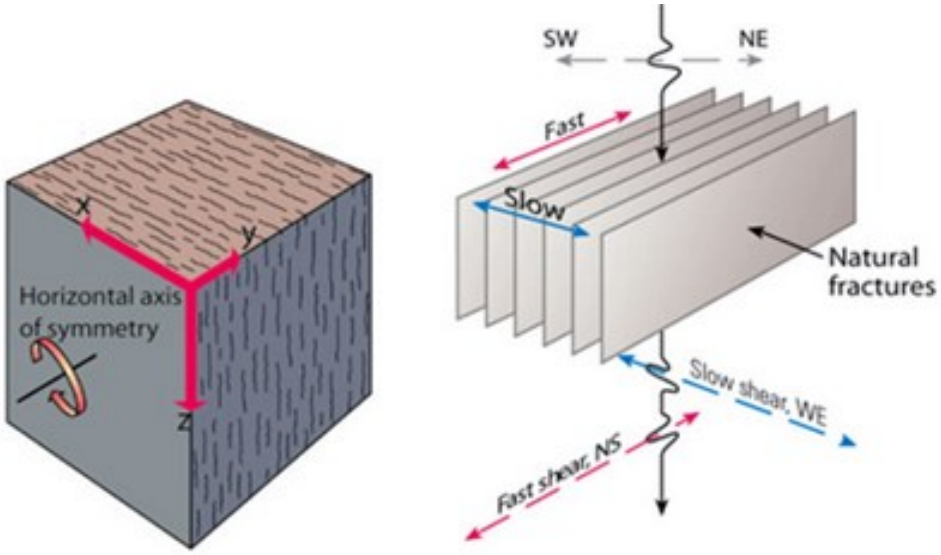

Figure 2:HTI model from vertical cracks

(The slow plane is in the direction perpendicular to the strike of the cracks with the fast plane lying parallel to the strike of the cracks. (After Close et al., 2009))

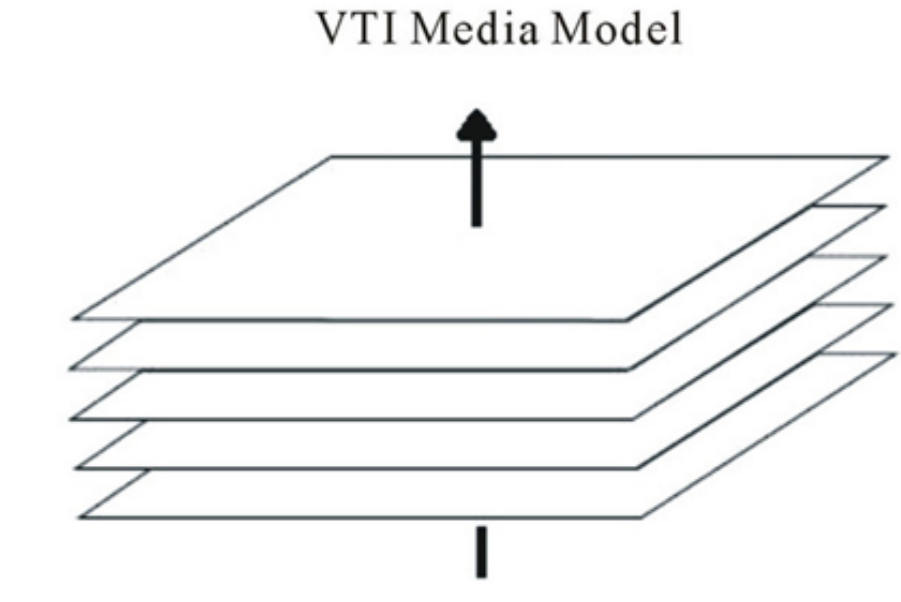

Figure 3: A simplified VTI model

The next section will be dealing with one symmetry class, the VTI and all the work and analysis will be done assuming this class of materials.

2.2. **Transverse Isotropy with Vertical axis of symmetry, VTI material**

The simplest anisotropic case of broad geophysical applicability has one distinct direction (usually, but not always, vertical), while the other two directions are equivalent to each other. This case- called transverse isotropy, or hexagonal symmetry (Thomsen, 1986). When the unique direction is vertical the material is said to be VTI. Material symmetry reduces the number of independent parameters, but this reduction is only applicable if the elastic stiffnesses are specified with respect to a coordinate system with axes aligned with the symmetry directions (Sayers, 1994).

Highest symmetry class is triclinic and it has 21 components. Lower symmetry class has fewer components. Orthorhombic symmetry has 8 components, the elastic stiffness tensor of a transversely isotropic material is invariant with respect to rotations about a symmetry axis and may be described by five independent elastic constants (Sayers, 1994). The VTI symmetry has therefore, only five independent non-zero components giving the elastic modulus matrix, $C_{\alpha\beta}$, the form

$$C_{\alpha\beta}=\begin{bmatrix} C_{11} & C_{11}-2C_{66} & C_{13} & 0 & 0 & 0 \\ 0 & C_{11} & C_{13} & 0 & 0 & 0 \\ 0 & 0 & C_{33} & 0 & 0 & 0 \\ 0 & 0 & 0 & C_{44} & 0 & 0 \\ 0 & 0 & 0 & 0 & C_{44} & 0 \\ 0 & 0 & 0 & 0 & 0 & C_{66} \end{bmatrix} \qquad (7)$$

Comparison of the isotropic matrix, equation (5), with the anisotropic matrix, equation (7), shows how the former is a degenerate special case of the latter, with (equation 8) (Thomsen, 1986)

$$\left.\begin{array}{c} C_{11}\rightarrow C_{33} \\ C_{66}\rightarrow C_{44} \\ C_{13}\rightarrow C_{33}-2C_{44} \end{array}\right\} \qquad (8)$$

Hence elements of the isotropy matrix can easily be obtained if its VTI matrix is known. While it's simple obtaining isotropic matrix from the VTI elastic modulus matrix the reverse is hardly achieved. (Thomsen, 1986) has observed that the generalization from isotropy to anisotropy introduces three new elastic moduli, rather than just one or two. This observation is fundamental to making decision which symmetry approximations to use while characterizing our reservoirs. Weak elastic anisotropy inform of VTI proves to be more suitable over its isotropic equivalent in this regard as switching to purely isotropy is possible rather than the reverse.

In particular, vertical and tilted transverse isotropy are currently treated as an integral part of velocity fields employed in prestack depth migration algorithms, especially those based on the wave equation (Tsvankin et al., 2010), this is an important observation to choosing VTI over other symmetries.

2.3. **Seismic upscaling and the Backus averaging**

The wave propagation in a homogeneous VTI medium can be described by a linear ordinary differential equation

$$\frac{d\boldsymbol{f}(z)}{dz} = i\omega \boldsymbol{M}\boldsymbol{f}(z) \qquad (9)$$

Where the vector $\mathbf{f}(z) = (\mathbf{v}, \boldsymbol{\tau})^T$ contains the velocity stress-strain components with the phase factor $\exp[i\omega(p_1 x + p_2 y - t)]$ defined for each layer and is a continuous function of depth z, $i = \sqrt{-1}$, ω is the angular frequency and system matrix $\mathbf{M}$ is defined by the horizontal slowness and the type of the medium (Gilbert and Backus, 1966). The matrix $\mathbf{M}$ is given as

$$\begin{pmatrix} A & C_{33}^{-1} \\ B & A^T \end{pmatrix} \qquad (10)$$

Here $\mathbf{A} = \mathbf{C}_{33}^{-1}(p_1\mathbf{C}_{31} + p_2\mathbf{C}_{32})$, $\mathbf{B} = \sum_{m,n=1,2} p_m p_n \left(\mathbf{C}_{m3}\mathbf{C}_{33}^{-1}\mathbf{C}_{3n} - \mathbf{C}_{mn}\right) + \rho\mathbf{I}$, $\mathbf{I}$ is the unit 3x3 matrix, and $\mathbf{C}_{mn}[p,q] = c_{mn,pq}$ is the matrix of stiffness coefficients (Stovas, Roganov, Duffaut, & Carter, 2013)

Sedimentary basins are composed of thinly laminated isotropic and/or anisotropic layers. For waves with wavelength longer than the individual layer thickness, Backus (1962) has demonstrated that the thin layers will be averaged and waves behave as if propagating in an effective-anisotropic homogeneous medium (Stovas and Arntsen, 2006).

Backus (1962) presented an elegant method of producing the effective constants for a thinly layered medium composed of either isotropic or anisotropic elastic layers (Berryman, 2005). It (Backus, 1962) gives an effective medium theory that replaces a rapidly varying, fine-layered earth model with one that is more homogeneous and long-wave equivalent to the original (Liner and Fei, 2006).

The Backus averaging gives the effective medium, the system matrix $\tilde{M}$ given by a simple arithmetic averaging of all system matrices from each of the thin individual layers. The theory is based on averaging in the context of Hooke's law for VTI media (Liner and Fei, 2006).

This method applies either to spatially periodic layering or to random layering, by which we mean either that the material constants change in a non-periodic (unpredictable) manner from layer to layer or that the layer thicknesses might also be random (Berryman, 2005). The conceptual approach of Backus is to write down expressions for stress and strain in each individual layer, then to consider averages over the entire stack of layers (Liner and Fei, 2006)

Given a layered and equally spaced VTI medium with N layers, $\tilde{M}$ is given as

$$\widetilde{\boldsymbol{M}} = \langle \boldsymbol{M} \rangle = \frac{\mathbf{1}}{\boldsymbol{N}} \sum_{j=1}^{N} \boldsymbol{M}_j \qquad (11)$$

Elements of matrices $\mathbf{M}_j$ for each layer, j from logging data for example, are computed from the standard Thomsen (1986) notations given as;

$$\left.\begin{array}{c} \mathrm{C}_{33j} = \rho_j v_{pj}^2 \\ \mathrm{C}_{44j} = \rho_j v_{sj}^2 \\ \mathrm{C}_{11j} = \mathrm{C}_{33j}(1 + 2\varepsilon_j) \\ \mathrm{C}_{13j} = \sqrt{(\mathrm{C}_{33j} - \mathrm{C}_{44j})(\mathrm{C}_{33j}(1 + 2\delta_j) - \mathrm{C}_{44j}) - \mathrm{C}_{44j}} \\ \mathrm{C}_{66j} = \mathrm{C}_{44j}(1 + 2\gamma_j) \end{array}\right\} \qquad (12)$$

The effective VTI medium is then formed and is a long wave equivalent of all the constituent layers, its stiffness coefficients and density properties can be computed from the elements of matrix $\widetilde{\mathbf{M}}$ defined in equation (12) using Backus averaging expressions with $\langle . \rangle$ being the arithmetic averaging operator as given in (11).

A definition of the properties of the effective medium, here with very minor modifications; is given by (Backus, 1962)in which he states that the density of the long wave equivalent medium is the average density and its elastic coefficients are algebraic combinations of averages of algebraic combinations of the elastic coefficients of the original medium. The expressions he obtained for the properties of the effective medium are given in equation (13)

$$\left.\begin{array}{c} \mathrm{C}_{\mathbf{11}} = \left\langle \mathrm{C}_{11} - \dfrac{\mathrm{C}_{13}^2}{\mathrm{C}_{33}} \right\rangle + \left\langle \dfrac{\mathrm{C}_{13}}{\mathrm{C}_{33}} \right\rangle^2 \langle \mathrm{C}_{33}^{-1} \rangle^{-1} \\ \mathrm{C}_{\mathbf{13}} = \left\langle \dfrac{\mathrm{C}_{13}}{\mathrm{C}_{33}} \right\rangle \langle \mathrm{C}_{33}^{-1} \rangle^{-1} \\ \mathrm{C}_{\mathbf{33}} = \langle \mathrm{C}_{33}^{-1} \rangle^{-1} \\ \mathrm{C}_{\mathbf{44}} = \langle \mathrm{C}_{44}^{-1} \rangle^{-1} \\ \mathrm{C}_{\mathbf{66}} = \langle \mathrm{C}_{66} \rangle \\ \boldsymbol{\rho} = \langle \rho \rangle \end{array}\right\} \qquad (13)$$

The standard VTI medium parametrization requires computation of the vertical P- and S-wave velocities and anisotropy parameters (as shown in equation 14) in Thomsen (1986) notation from the elements of the effective stiffness matrix in equation (13).

These parameters (three parameters Epson (ε), delta (δ) and gamma (γ)), describing the variation of compressional and shear velocities as a function of polar angle with respect to the symmetry axis, are very useful in quantifying the degree of anisotropy (Collet and Gurevich, 2013). The vertical velocities, both for compressional and shear waves are important inputs for calculating the moveout velocity required in seismic processing of compressional and shear waves respectively. While applying the Backus averaging on VTI layers, the result is an effective medium that is also VTI.

$$\left.\begin{aligned} \mathcal{V}_P &= \sqrt{\frac{\mathbf{C_{33}}}{\boldsymbol{\rho}}} \\ \mathcal{V}_S &= \sqrt{\frac{\mathbf{C_{44}}}{\boldsymbol{\rho}}} \\ \varepsilon &= \frac{\mathbf{C_{11}} - \mathbf{C_{33}}}{2\mathbf{C_{33}}} \\ \gamma &= \frac{\mathbf{C_{66}} - \mathbf{C_{44}}}{2\mathbf{C_{44}}} \\ \delta &= \frac{(\mathbf{C_{13}} + \mathbf{C_{44}})^2 - (\mathbf{C_{33}} - \mathbf{C_{44}})^2}{2\mathbf{C_{33}}(\mathbf{C_{33}} - \mathbf{C_{44}})} \end{aligned}\right\} \qquad (14)$$

2.4. Fluid substitution

Fluid changes in the rock have an influence on the basic reservoir properties hence affect the signal from seismic data. The effects on seismic data of fluid changes are attributed to changes in rock stiffness and density. Gassmann's equation predicts that for an isotropic rock, the rock bulk modulus will change if fluid changes while the shear modulus will not (Avseth et al., 2005). Given a change from a dry phase to a fluid saturated phase the bulk modulus for as presented in (Avseth et al., 2005), is

$$\frac{K_{sat}}{K_{mineral} - K_{sat}} = \frac{K_{dry}}{K_{mineral} - K_{dry}} + \frac{K_{fluid}}{\emptyset(K_{mineral} - K_{fluid})} \qquad (15)$$

And the companion equation given as

$$\mu_{sat} = \mu_{dry} \qquad (16)$$

Where

K_{sat} is the fluid saturated bulk modulus, $K_{mineral}$ is the bulk modulus for the solid grains, K_{dry} is the bulk modulus for the framework (grains + matrix), K_{fluid} is the bulk modulus for the saturating fluid, $\emptyset$ is the total porosity, μ_{sat} is the shear modulus for the saturated phase while μ_{dry} is the shear modulus for the dry phase.

When dealing with fluid substitution problems where one fluid, fluid1, is being replaced with another fluid, fluid2, a direct approach of applying Gassmann's fluid substitution equation for bulk modulus would be as given in (17)

$$\frac{K_{sat2}}{K_{mineral} - K_{sat2}} - \frac{K_{fluid2}}{\emptyset\left(K_{mineral} - K_{fluid2}\right)}$$

$$= \frac{K_{sat1}}{K_{mineral} - K_{sat1}} - \frac{K_{fluid1}}{\emptyset\left(K_{mineral} - K_{fluid1}\right)} \qquad (17)$$

While the shear modulus remains constant in the two scenarios;

$$\mu_{sat2} = \mu_{sat1} \tag{18}$$

WhereK_{sat1} and K_{sat2} and are the rock bulk moduli saturated with fluid1 and fluid2 and $K_{fluid1}$and K_{fluid2} are the bulk moduli for the fluids themselves (Avseth et al., 2005).

The bulk moduli for the dry and saturated phases are related to P-wave and S-wave velocities as in equation (19),

Where ρ is the bulk density and is defined below;

$$\left\{\begin{array}{c} v_p = \sqrt{\dfrac{K + (4/3)\mu}{\rho}} \\ v_s = \sqrt{\mu/\rho} \\ \rho = \Phi\rho_{fluid} - (1-\Phi)\rho_{mineral} \end{array}\right\} \tag{19}$$

Hydrocarbon bearing reservoirs are not fully saturated with only one fluid type. A proper fluid substitution is therefore required that would take into consideration different fluids present in the reservoir. Gassmann's relations were originally derived to describe changes in rock modulus from one pure saturation to another-from dry to fully brine-saturated, from fully brine-saturated to fully oil-saturated, etc. (Avseth et al., 2005). Equation for determining the coefficient of stiffness (bulk modulus) for a mixture of fluids has been derived by Domenico (1976) by replacing the fluid mixture with an effective fluid having bulk modulus, $\bar{K}_{fluid}$. The relation is given as in equation (20)

$$\left\{\begin{array}{c} \dfrac{1}{\bar{K}_{fluid}} = \dfrac{S_{gas}}{K_{gas}} + \dfrac{S_{oil}}{K_{oil}} + \dfrac{S_{br}}{K_{br}} = \left\langle \dfrac{1}{K_{fluid}(x,y,z)} \right\rangle \\ \rho fluid = S_{gas}\rho_{gas} + S_{oil}\rho_{oil} + S_{br}\rho_{br} = \langle \rho_{fluid}(x,y,z) \rangle \end{array}\right\} \tag{20}$$

Where

$S_{gas,oil,br}$, $K_{gas,oil,br}$ and $\rho_{gas,oil,br}$ are the saturations, bulk moduli and densities of gas, oil and brine phases. The operator $\langle . \rangle$ refers to a volume average and allows for more compact expressions (Avseth et al., 2005).

Where $K_{fluid}(x, y, z)$ and $\rho_{fluid}(x, y, z)$ are the spatially varying pore-fluid modulus and density (Avseth et al., 2005).

Gassmann's relations are strictly valid only for isotropic rocks. Real rocks are always at least slightly anisotropic, making Gassmann's relations inappropriate in the strictest sense (Avseth et al., 2005). It has long been recognized that elastic waves in layered media are likely to have an anisotropic velocity distribution for wavelengths long compared to the spacing of the layers (Berryman, James G., 1979) and therefore applying isotropic assumptions in characterizing our reservoirs does not provide an accurate astimate of the properties in question. (Mavko and Bandyopadhyay, 2009) have shown that the use of isotropic approximations sometimes over predicts the actual fluid response while it underestimates them in some others, resulting in incorrect interpretation of seismic attributes for fluid detections (Li, 2013). The approximate expression derived for fluid substitution for waves travelling in the vertical axis in a Transverse Isotropy with the vertical axis of symmetry by (Mavko and Bandyopadhyay, 2009) is not valid for rocks with very high anisotropies or when the porosity is low providing another challenge of knowing the anisotropic extent (degree of anisotropy) prior to applying this approximate expression as it may lead to catastrophic error.

Nevertheless, the best approach, given the limited data available in the field, is to use Gassmann's relations on measured Vp and Vs (and density) even though the rocks are anisotropic (Avseth et al., 2005). Also, most unfractured reservoir rocks (as assumed in this case) are nearly intrinsically isotropic, unless they contain substantial amounts of clays or are

finely layered (Wang, 2002) making isotropic substitution a reasonable approximation to the properties of the reservoir. Therefore, isotropic assumption, though not very perfect, has been studied and found to provide parameters that nearly characterize most subsurface features of interest in exploration geophysics. During this study the isotropic Gassmann's relations were assumed for fluid substitutions for well log data at different fluid saturations.

3. Results

Results have been organized into five different categories corresponding to five reservoir properties that characterize the effective VTI medium. Graphs are presented for each property at different fluid saturations, Figure 4 to Figure 9 for all 40 blocks. Tables for all the properties are attached as appendix 8.

The vertical P wave velocity calculated is observed to be constant for different fluid saturations at some intervals (Figure 1). Few intervals with changes in the velocity are reservoir sections, named with increasing depth from top, block number 10, 15, 18, 22, 32 and 36. The effect of gas substitution in lowering the P-wave velocity for an effective medium is more significant for shallow reservoirs in which the velocity in gas saturated effective medium is less than in oil saturated medium than it is for deeper reservoirs.

In most of the deeper reservoirs, below block 19 (depth-3024m) gas and oil have approximately the same effect on P-wave velocity for the effective medium.

The results also show that the measured data and the data corresponding to 100% water saturation have the same velocity in all blocks as shown between the curves corresponding to Vp0_measured and Vp0_wet in Figure 1 respectively, the velocity of which is higher than the velocity in oil.

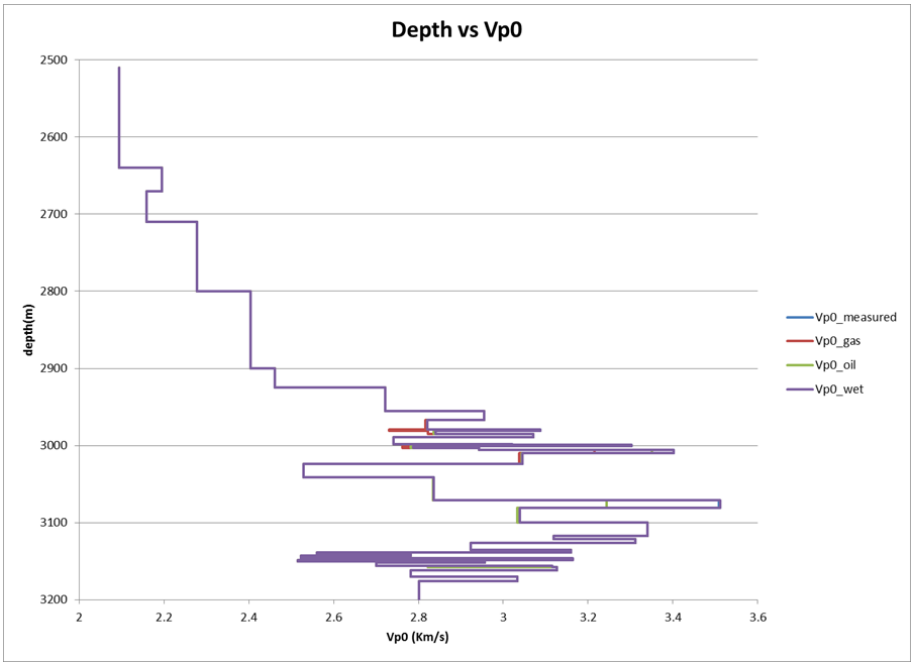

Figure 4: Vp0 at different fluid saturations

Figure 5 shows the shear wave velocity for the effective medium plotted for all 40 resultant blocks. No significant changes are observed for shear wave velocity for all the blocks at different saturations. Very minor changes on reservoir sections occur.

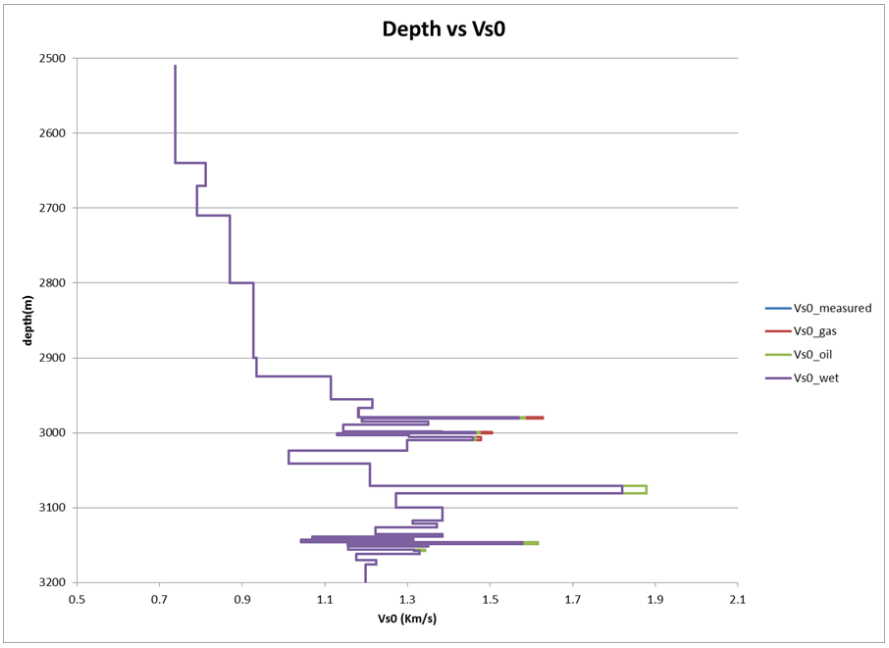

Figure 5: Vs0 at different fluid saturations

Gamma is observed to remain constant at each depth interval for the different saturations for all the 40 blocks (Figure 6).

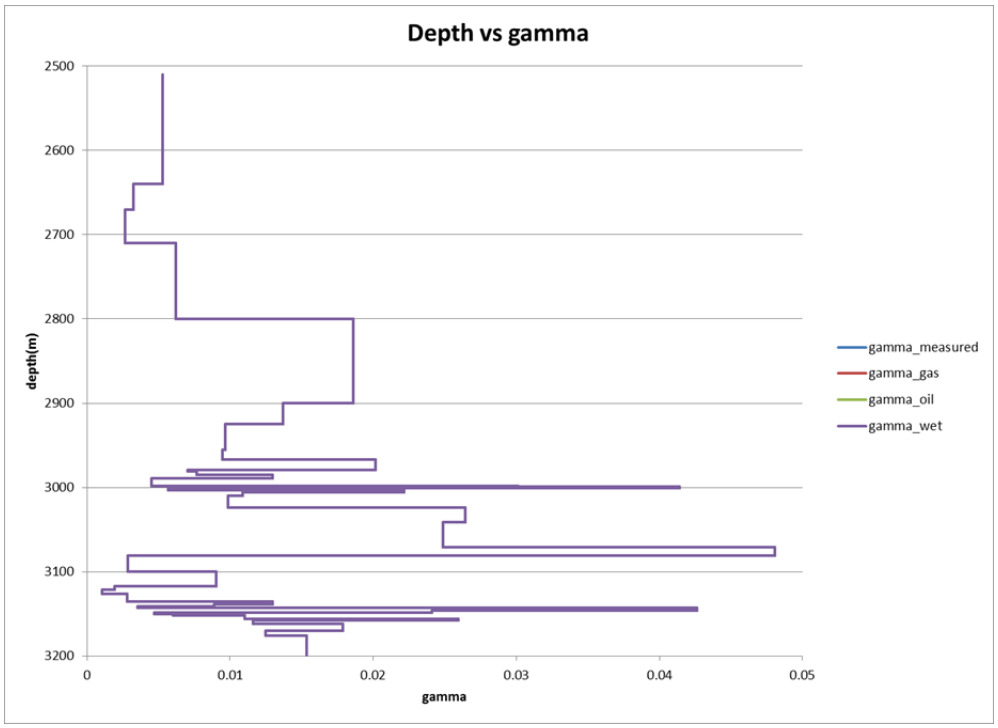

Figure 6: gamma at different fluid saturations

The P-wave parameter, epsilon appears to change over several points for those blocks adjacent to reservoirs and on reservoir sections for the different fluid saturations (Figure 7). Epsilon parameter obtained from the measured and water saturated effective media are the same as it has been for the P-wave velocity. The difference in parameter between measured, oil and gas saturated media is not uniform. Some reservoir sections (blocks) see same ε-value for the oil and gas saturated media. Gas saturated effective medium is generally observed to be more anisotropic than is the case for water and oil saturated media. Generally the trend can be divided into two pairs, the first pair is density-oil group and the second is the measured-water pair. For shallower reservoirs above a depth of 3170m the first pair has different values between them at each depth and the gas saturated medium has a higher absolute value of epsilon compared to oil saturated medium. Below 3170m (below block 20) the two media

have same values at their corresponding depth. The second pair has at every corresponding depth approximately same value of the P-wave anisotropy between the measured and water saturated media. In all sections where the value of the P-wave anisotropy between the different saturated media is different, the Epson value decreases from gas media then oil media and water media has the lowest absolute value.

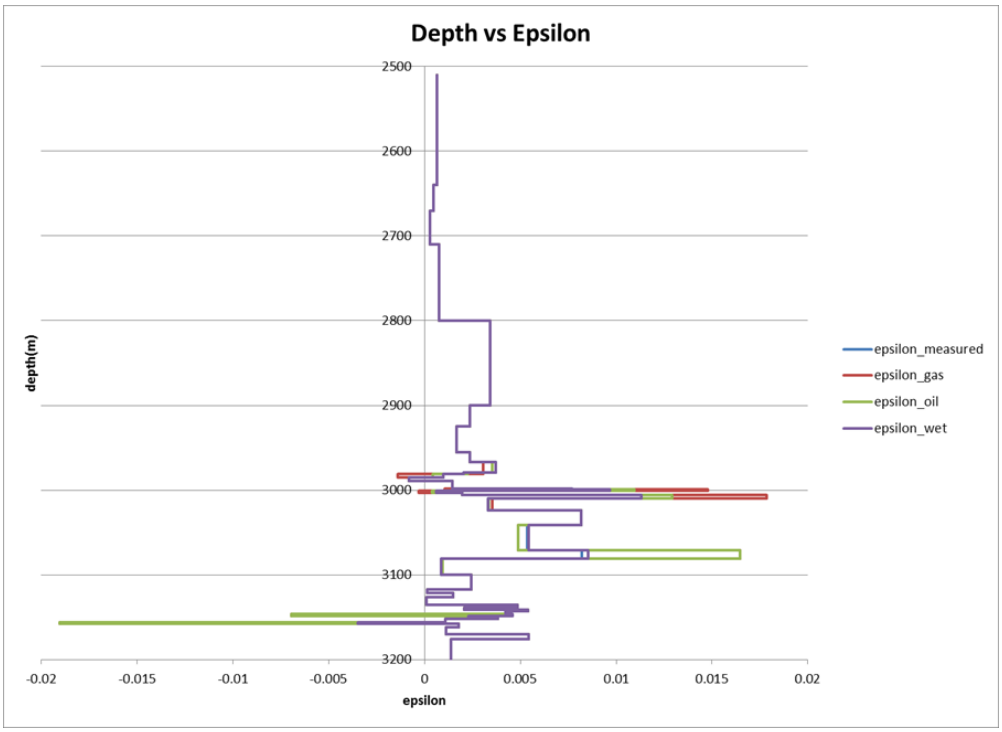

Figure 7: epsilon at different fluid saturations

Delta values display a pattern characteristic which can be divided into two parts (Figure 8), one corresponding to the top section down to block number 16 (depth-3003m). This part is characterized by same delta values at the most top blocks for all fluid saturations which then changes slightly in those blocks that make reservoirs and a significant deviation in values from the rest of the delta value for the gas saturated media in those blocks that appear before or adjacent to reservoir blocks. Second part which encompasses the deep blocks starting from block number 17 (depth-3006m) is characterized by a more deviating delta value from gas and oil saturated media as compared to measured and water saturated media in reservoir

blocks. The last two cases (measured and water saturated) have similar values in all blocks. The gas-oil pair similarity in delta values occur in all blocks except in block number 18 where delta value from the gas saturated effective medium is greater than its corresponding value from the oil saturated medium. In all blocks where delta values are different for the different fluid saturations, gas saturated medium has a highest absolute value followed by oil except in block 22 (depth-3081.2m) where the measured-water saturated delta value is higher than the gas-oil saturated pair value.

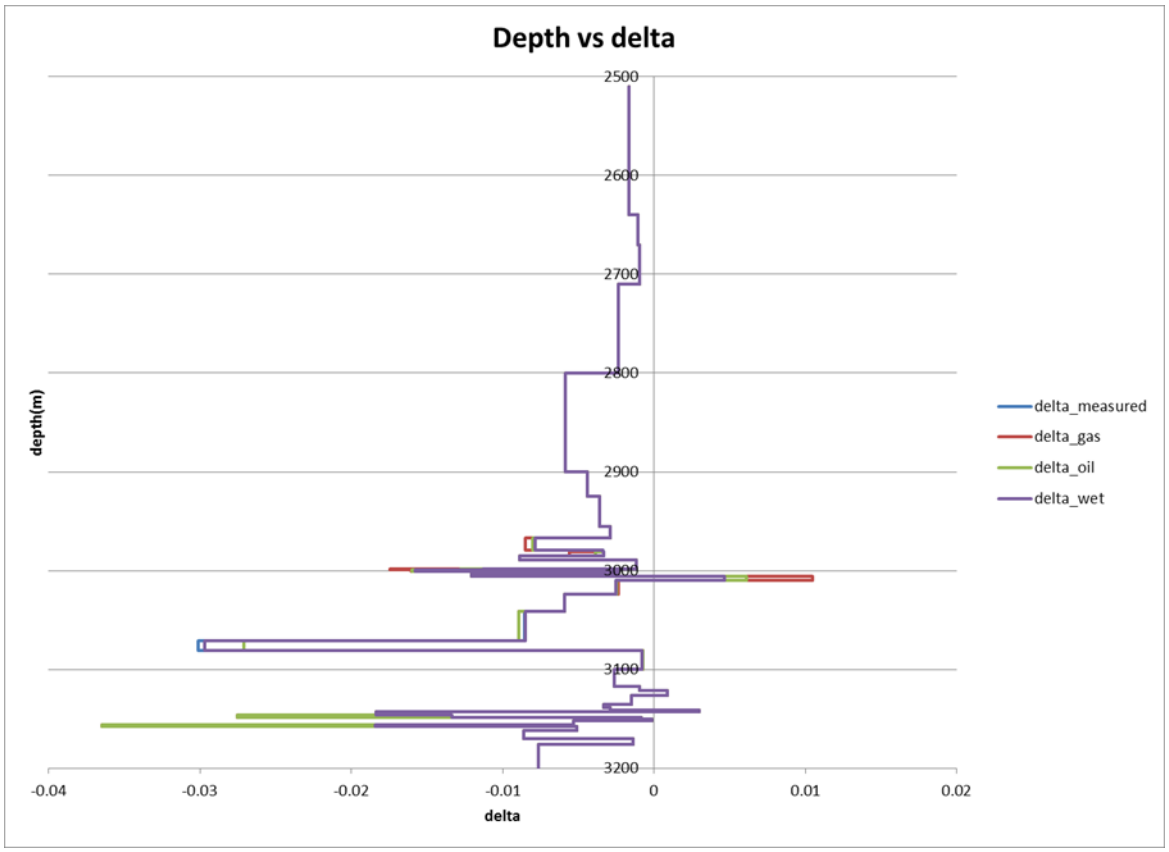

Figure 8: delta at different fluid saturations

4. Discussion

Vertical P-wave velocity depends on stiffness coefficient, C_{33} and density of the effective medium. The differences in velocity (in figure 4) stems from the fact that the different fluids have different densities and therefore when substituted in the medium they also have different effects on the bulk stiffness coefficient and density. At all intervals (shallow reservoir sections) where the velocities of the different saturated media are different, there is a general increase in velocity from gas-, oil- to water-saturated effective medium. This is consistent with the conclusion made by (Toksoz, Cheng, & Timur, 1976) that the dry and gas saturated samples have lower moduli as compared to oil and brine saturated samples. The velocities are following the same order and from (Toksoz, Cheng, & Timur, 1976) this could infer the shape of the pore spaces as being flatter. For deeper reservoirs, the gas- and oil-saturated media have similar velocity which implies that the rocks are becoming stiffer such that the less dense gas and oil have a comparable effect in affecting the bulk elastic coefficients and density of the effective medium. The similarity in velocity between the measured and water saturated media explains the fluid composition of the measured reservoir intervals in the well in which case, their pore spaces are all filled with water.

The shear modulus is observed to remain constant or vary negligibly between the different saturations in figure 5, as the shear modulus is very little affected or not affected by the saturating fluid. (Thomsen, 2012) has observed that both S44 and S66 are independent of fluid content. Where S stands for compliance.

Since the shear stiffnesses, C44 and C66 are simply the inverses of the corresponding compliances, it follows that both C44 and C66 are independent of fluid content (Thomsen, 2012).

A small variation observed is derived from density whereby, gas being less dense when substituted reduces the bulk density thereby increasing the S-wave velocity to a small extent as observed in figure 5. The other causes might be as suggested by (Khazanehdari & Sothcott, 2003) to be viscous coupling, reduction in free surface energy, and, to a limited extent, frequency dispersion due to both local and global flow.

Gamma being the shear wave splitting parameter is given as the ratio of two shear wave velocities. Since the shear wave velocity (figure 5) is very little and almost not affected by fluid saturation it is not surprising to see the shear wave splitting parameter to remain constant irrespective of the fluid that has been substituted into the pores (figure 6). (Collet and Gurevich, 2013) and (Thomsen, 2012) have made similar observations owing to shear modulus not or little being affected by the saturating fluids.

The P-wave anisotropy is not constant over the whole interval despite doing so at some depth intervals. Constant epsilon value appear on non-reservoir sections indicating that the no-porosity regions contain no or less fluid and therefore fluid substitution in not effective leaving the gross reservoirs properties unchanged. Some non-reservoir sections that are overlying or underlying reservoir sections see change in epsilon value. This might be due to the partial fluid substitution at the boundary between them and their underlying or overlying reservoirs respectively due to the grading lithological boundaries or inaccuracies in the logging scheme that marked tops of lithologies.

Changes on reservoir sections which are attributed to changes in rock stiffness and density form a characteristic pattern of two pairs. The first pair is density-oil group and the second is the measured-water pair. For shallower reservoirs above 3170m the first pair has different values between them at each depth and the gas saturated medium has a higher absolute epsilon values compared to oil saturated medium. This can be accounted for by the fact that

reservoir compaction due to overburden stress increases with depth. Given same environmental of deposition, the shallower reservoirs are expected to be less stiff as compared to deeper reservoirs. The fluid effect is therefore expected to be more pronounced in shallower reservoirs even for gas and light oil which have comparable effect in affecting the gross reservoir properties due to a small density difference between them. As it has been observed by (Gregory, 1975) 'replacing pore liquids with gas markedly reduces the elastic moduli of rocks, and the effect is enhanced by decreasing pressure'. Therefore gas has more effect on reservoir properties as compared to oil as observed implying that it is possible to discriminate between gas and oil on seismic sections. Below 3170m (below block 20) the two media have same values at their corresponding depth due to the low influence of both gas and oil as the rock becomes more stiff such that the stiffness coefficient from the matrix dominates the fluid effect and therefore the two fluids will have the same effect on seismic sections and cannot be qualitatively discriminated. A study conducted by (Wang, 2002) on sedimentary rocks has revealed that 'tight sands, shaly sands, siltstones, or thin sand–shale sequences may be seismically anisotropic. The anisotropy may exceed 10% in these rocks'. This might be what is happening in the deeper reservoirs causing higher degree of anisotropy masking the effect of oil and gas substitutions, the result of which is these fluids having the same degree of anisotropy as can be seen in figure 7.

The second pair has at every corresponding depth same value of the P-wave anisotropy between the measured and water saturated media. This explains itself that the measured dataset media is the same as the water saturated media and therefore the reservoirs are all water saturated. Gas, as observed has higher absolute values as compared to other fluids. This is consistent with observation made by (Collet and Gurevich, 2013). They observed that the degree of P-wave anisotropy is reduced by the presence of fluid implying fluids are less anisotropic but the degree of isotropy differs between gas, oil and water. 'The less

compressible the fluid, i.e., the higher the fluid bulk modulus Kf, the more affected the degree of anisotropy' (Collet and Gurevich, 2013).

Delta parameter represents a quasi P-wave anisotropy meaning it is not purely a P-wave parameter as it involves shear wave components interms of the stiffness coefficients C_{13} and C_{44}. The variation with fluid saturation of delta values is complex as compared to epsilon values. The general trend resembles the P-wave anisotropy and the absolute value of delta from the gas saturated effective medium is higher compared to other fluid saturated effective media for shallow reservoirs above block 19 (depth-3024m). Below this depth oil and gas saturated effective media have approximately the same delta values, the absolute value of which is higher than the delta value from the measured and water saturated effective media except in block 22 (depth, 3070.8m-3081.2m) in which the measured and water saturated value is higher than the oil-gas pair value.

It is well known that the shear stiffness coefficients are not or little affected by the saturating fluids. This implies that most of the fluid effect in delta values is derived from the compressional stiffness coefficients and in this case, C_{33}. Derivations by Thomsen (2012) for the fluid effect on ε and δ has shown that both are dependent on the incompressibility of the pore fluid concluding that the anellipticity constant, eta is invariant of fluid saturation. The other equation by the same author (he suggests being more exact) is hard to grasped intuitively. However, the inconsistency in delta and epsilon value in block 22 (depth, 3070.8-3081.2m) as observed brings a challenge into concluding that both epsilon and delta have the same fluid effect response. The presence of the shear component C_{13} and C_{44} on delta might be one the factors.

5. Conclusion

Wave propagation through a layered earth is a complex physico-chemical phenomenon which cannot be simply modelled by the simplest isotropic assumptions. Gassmann's isotropic fluid substitution equation does not provide the most exact solution but the assumptions provide approximate parameters that can aid characterization of the layered earth.

Anisotropy approximation informs of the Transverse Isotropy with a Vertical axis of symmetry (VTI) provides a better estimate of the properties of subsurface compared to their isotropic counterpart. The parameters characterizing the VTI medium have different responses to fluids present in the pore spaces. Vertical P-wave velocity (Vs0) as observed from data used in this study is higher in water saturated compared to oil and gas saturated effective media, the velocity in the gas saturated effective medium being the lowest.

Vertical Shear wave velocity (Vs0) is approximately invariant of fluid substitution. A slight increase in velocity is observed when the light fluid is in the pores. The anisotropy parameter, γ is invariant of fluid substitution.

The P-wave anisotropy, ε is higher in gas than oil in shallower reservoirs above 3170m. Oil derived ε is higher than the water derived value. The epsilon value from gas and oil derived effective media are the same in all deeper reservoirs.

The epsilon parameter has a general trend of response as epsilon except in block 22. This implies the general conclusion that eta is invariant of fluids present in the pores in not always valid.

In all fluid cases, water saturated effective medium and an effective medium derived from the measured data have similar values at each corresponding depth even on reservoir sections. This means all reservoir sections penetrated by the well are water saturated.

6. Recommendations

This work is based (entirely) on one well data. This reduces the reliability of the findings and conclusion. In order to have more reliable findings, it is hereby recommended that;

1. A study involving multiple wells from the same place be conducted. The results have to be compared to another similar work done on a different area.

2. The variation of delta with fluid saturation seems to more complex than earlier perceived, a detailed work involving mathematical formulation has to be conducted that will enable establishment of the explicit relationship between fluid saturation and delta based on field or experimental data.

7. References

Liner and Fei. (2006). Layer-induced seismic anisotropy from full-wave sonic logs:Theory, application, and validation. *GEOPHYSICS, Vol. 71*(No. 6), D183–D190.

Stovas and Arntsen. (2006). Vertical propagation of low-frequency waves in finely layered media. *Geophysics, Vol. 71*(No. 3), T87–T94.

Avseth et al. (2005). *Quantitative seismic interpretation. Applying a rock physics tools to reduce interpretation risks.* Cambridge: Cambridge University Press.

Backus, G. E. (1962). Long-Wave Elastic Anisotropy Produced by Horizontal Layering. *Journal of Geophysical research, Volume 67*(No. 11).

Batzle and Wang. (1992). Seismic properties of pore fluids. *Geophysics, Vol. 57*(No. 11), 1396-1408.

Berryman, J. G. (2005). Fluid effects on shear waves in finely layered porous media. *Geophysics, Vol. 70*(No. 2), N1-N15.

Berryman, James G. (1979). Long-wave elastic anisotropy in transversely isotropic media. *Geophysics. Vol. 44. No. 5*, 896-917pp.

Close, D., Cho, D., Horn, F., & Edmundson, H. (2009). The Sound of Sonic: A Historical Perspective and Introduction to Acoustic Logging. *CSEG Recorder, 34*(05), 34-43.

Collet and Gurevich. (2013). Fluid dependence of anisotropy parameters in weakly anisotropic porous media. *Geophysics, Vol. 78*(No. 5), WC137–WC145.

Gilbert and Backus. (1966). Propagator matrices in elastic waves and vibration problems. *Geophysics, Vol XXXI*(No. 2), 326-332.

Gregory, A. (1975). Fluid saturation effects on dynamic elastic properties of sedimentary rocks. *45th Annual International SEG meeting* (pp. 895-921,). Denver: Society of Exploration Geophysicists.

Khazanehdari, J., & Sothcott, J. (2003). Variation in dynamic elastic shear modulus of sandstone upon fluid saturation and substitution. *Geophysics, 68*(2), 472-481.

Li, S. (2013). Physical modelling and the poroelastic model with application to fluid detection in a VTI medium. *Journal of Geophysics and Engineering, J. Geophys. Eng.*(10), 11.

Mavko and Bandyopadhyay. (2009). Approximate fluid substitution for vertical velocities in weakly anisotropic VTI rocks. *Geophysics, Vol. 74*(No. 1), D1-D6.

Norris and Sinha. (1993). Weak elastic anisotropy and the tube wave. *Geophysics, Vol. 58*(No. 8), 1091-1098.

Ruger, A. (1998). Variation of P-wave reflectivity with offset and azimuth in anisotropic media. *Geophysics, Vol. 63*(No.3), 935-947.

Sayers, C. M. (1994). P-wave propagation in weakly anisotropic media. *Geophysics Journal International,*(116), 799-805.

Stovas, A., Roganov, Y., Duffaut, K., & Carter, A. J. (2013). Low-frequency layer-induced anisotropy. *Geophysics, Vol. 78*(No. 5), WC3–WC14.

Thomsen, L. (1986). Weak elastic anisotropy. *Geophysics, Vol, 51*(No. 10), 1954-1966.

Thomsen, L. (2012). On the fluid dependence of the parameters of anisotropy. *SEG Las Vegas 2012 Annual Meeting* (pp. 1-5). Las Vegas: SEG.

Toksoz, M. N., Cheng, C. H., & Timur, A. (1976). Velocities of seismic waves in porous rocks. *Geophysics, 41*(4), 621-645.

Tsvankin et al. (2010). Seismic anisotropy in exploration and reservoir characterization: An overview. *Geophysics,Vol. 75, No. 5*, 75A15–75A29pp.

Wang, Z. (2002). Seismic anisotropy in sedimentary rocks, part 2: Laboratory data. *Geophysics, 67*(05), 1423–1440.

Wang, Z. (2002). Seismic Anisotropy in Sedimentary Rocks, part 2: Laboratory data. *Geophysics, Vol. 67, No. 5*, 1423–1440pp.

8. Appendices

Appendix A: Table showing block number assignment to depth intervals forming effective medium

Depth from (m)	Depth to (m)	Block number
2510.4	2640	1
2640	2670	2
2670	2710	3
2710	2800	4
2800	2900	5
2900	2925	6
2925	2955	7
2955	2967	8
2967	2979	9
2979	2981	10
2981	2985	11
2985	2989	12
2989	2998	13
2998	2999	14
2999	3001	15
3001	3003	16
3003	3006	17
3006	3010	18
3010	3024	19
3024	3041	20
3041	3070.8	21
3070.8	3081.2	22
3081.2	3100	23
3100	3117	24
3117	3121	25
3121	3126	26
3126	3135	27
3135	3139	28
3139	3141.5	29
3141.5	3143	30
3143	3146	31
3146	3148.5	32
3148.5	3150	33
3150	3152	34
3152	3156	35
3156	3158	36
3158	3162	37
3162	3170	38
3170	3176	39
3176	3200	40

Appendix B: Calculated vertical P-wave velocity for different fluid saturations

Blocks	Vp0_measured	Vp0_gas	Vp0_oil	Vp0_wet
1	2.0946053021224	2.0946052348879	2.0946052348976	2.0946052348976
2	2.1952155068373	2.1952154368597	2.1952154368597	2.1952154368597
3	2.1587251602355	2.1587250910073	2.1587250910073	2.1587250910073
4	2.2772380801474	2.2772380074686	2.2772380074686	2.2772380074686
5	2.4049293633087	2.4049292862709	2.4049292862709	2.4049292862709
6	2.4619373585694	2.4619372797395	2.4619372797395	2.4619372797395
7	2.7211479925459	2.7211479056213	2.7211479056213	2.7211479056213
8	2.9552709902408	2.9552708966793	2.9552708966793	2.9552708966793
9	2.8215302905608	2.8160423502008	2.8202428460480	2.8215302002315
10	3.0870652128887	2.7302623338644	2.9819483576519	3.0870651138289
11	2.8405601987002	2.8222738467578	2.8363092313146	2.8405601069812
12	3.0710839067634	3.0710838080252	3.0710838080252	3.0710838080252
13	2.7414956049455	2.7414955173317	2.7414955173317	2.7414955173317
14	3.0205792072265	2.9930099424860	3.0136709774964	3.0205791115869
15	3.3017449643072	2.9489017488674	3.1979265791284	3.3017448578015
16	2.7880531970394	2.7620844718627	2.7817340436445	2.7880531070295
17	2.9435040847998	2.9435039904716	2.9435039904716	2.9435039904716
18	3.4017299513336	3.2152386574424	3.3501034127023	3.4017298432776
19	3.0450863395871	3.0370153819105	3.0431622321562	3.0450862423312
20	2.5297876490736	2.5297875679506	2.5297875679506	2.5297875679506
21	2.8355583340575	2.8348549317509	2.8348549317509	2.8356352470271
22	3.5083621138489	3.2431877442767	3.2431877442767	3.5111440409930
23	3.0392470519261	3.0338140362108	3.0338140362108	3.0392469548630
24	3.3402329153847	3.3402328090013	3.3402328090013	3.3402328090013
25	3.1188181194450	3.1188180200081	3.1188180200081	3.1188180200081
26	3.3116019132907	3.3116018070234	3.3116018070234	3.3116018070234
27	2.9228406474040	2.9228405541782	2.9228405541782	2.9228405541782
28	3.1593433912284	3.1593432902286	3.1593432902286	3.1593432902286
29	2.5603797788827	2.5603796981819	2.5603796981819	2.5603796981819
30	2.7821067645805	2.7821066764774	2.7821066764774	2.7821066764774
31	2.5237675191507	2.5237674383633	2.5237674383633	2.5237674383633
32	3.1534619874398	2.9111877337807	2.9111877337807	3.1643718430127
33	2.5150028280440	2.5150027472300	2.5150027472300	2.5150027472300
34	2.9556464172676	2.9556463229192	2.9556463229192	2.9556463229192
35	2.7008943007006	2.7008942135718	2.7008942135718	2.7008942135718
36	3.1080465851270	2.8228476462321	2.8228476462321	3.1162150355497
37	3.1262705054898	3.1262704066917	3.1262704066917	3.1262704066917
38	2.7819161701428	2.7819160812101	2.7819160812101	2.7819160812101
39	3.0333693794163	3.0333692829751	3.0333692829751	3.0333692829751
40	2.8007141789652	2.8007140893554	2.8007140893554	2.8007140893554

Appendix C: Calculated S-wave velocity for different fluid saturations

Blocks	Vs0_measured	Vs0_gas	Vs0_oil	Vs0_wet
1	0.7381194864947	0.7381194628735	0.7381194628733	0.7381194628733
2	0.8112943857736	0.8112943596804	0.8112943596804	0.8112943596804
3	0.7900427567018	0.7900427313552	0.7900427313552	0.7900427313552
4	0.8705323491733	0.8705323211943	0.8705323211943	0.8705323211943
5	0.9269706514467	0.9269706218687	0.9269706218687	0.9269706218687
6	0.9348848337844	0.9348848036869	0.9348848036869	0.9348848036869
7	1.1151193246106	1.1151192888891	1.1151192888891	1.1151192888891
8	1.2152345862192	1.2152345470334	1.2152345470334	1.2152345470334
9	1.1812563335671	1.1817021479418	1.1813726297297	1.1812562956580
10	1.5691158797717	1.6277449847182	1.5838078770477	1.5691158281001
11	1.1892850224251	1.1907133773159	1.1896574050845	1.1892849844647
12	1.3499406437556	1.3499406006859	1.3499406006859	1.3499406006859
13	1.1451807300725	1.1451806935957	1.1451806935957	1.1451806935957
14	1.3824561097201	1.3853539053542	1.3832120835677	1.3824560650545
15	1.4649611876742	1.5055759382555	1.4752636179170	1.4649611392209
16	1.1303288459769	1.1327008797966	1.1309476985787	1.1303288072931
17	1.3045306569035	1.3045306146147	1.3045306146147	1.3045306146147
18	1.4589925144654	1.4786045328200	1.4640493936601	1.4589924678985
19	1.2993438476546	1.2998788720056	1.2994837764100	1.2993438063027
20	1.0120525256534	1.0120524930752	1.0120524930752	1.0120524930752
21	1.2098999162139	1.2100275827322	1.2100275827322	1.2098834219464
22	1.8207004024492	1.8783670069776	1.8783670069776	1.8199092796257
23	1.2723009379422	1.2726326086005	1.2726326086005	1.2723008969840
24	1.3844749143821	1.3844748698158	1.3844748698158	1.3844748698158
25	1.3121273182389	1.3121272760819	1.3121272760819	1.3121272760819
26	1.3715876623576	1.3715876183865	1.3715876183865	1.3715876183865
27	1.2228796025748	1.2228795636468	1.2228795636468	1.2228795636468
28	1.3852213867420	1.3852213436331	1.3852213436331	1.3852213436331
29	1.0702712888934	1.0702712547666	1.0702712547666	1.0702712547666
30	1.3145048964633	1.3145048550448	1.3145048550448	1.3145048550448
31	1.0432285843113	1.0432285512358	1.0432285512358	1.0432285512358
32	1.5807457917769	1.6157389998205	1.6157389998205	1.5791524264146
33	1.1545902133289	1.1545901764670	1.1545901764670	1.1545901764670
34	1.3509523237175	1.3509522814505	1.3509522814505	1.3509522814505
35	1.1560390479283	1.1560390099629	1.1560390099629	1.1560390099629
36	1.3165395251967	1.3421340478715	1.3421504113688	1.3154624311442
37	1.3290318893903	1.3290318475433	1.3290318475433	1.3290318475433
38	1.1760254737284	1.1760254366879	1.1760254366879	1.1760254366879
39	1.2245568299921	1.2245567902768	1.2245567902768	1.2245567902768
40	1.1980565645207	1.1980565266661	1.1980565266661	1.1980565266661

Appendix D: Calculated epsilon for different fluid saturations

Blocks	epsilon_measured	epsilon_gas	epsilon_oil	epsilon_wet
1	0.0006499753077	0.0006499753114	0.0006499753110	0.0006499753110
2	0.0004778559899	0.0004778559982	0.0004778559982	0.0004778559982
3	0.0002806849719	0.0002806849711	0.0002806849711	0.0002806849711
4	0.0007493899366	0.0007493899262	0.0007493899262	0.0007493899262
5	0.0034318032617	0.0034318032529	0.0034318032529	0.0034318032529
6	0.0023471878120	0.0023471878012	0.0023471878012	0.0023471878012
7	0.0016834244351	0.0016834244440	0.0016834244440	0.0016834244440
8	0.0023638405695	0.0023638405426	0.0023638405426	0.0023638405426
9	0.0037082710291	0.0030423485669	0.0035495838828	0.0037082710548
10	0.0020378855339	0.0030649767767	0.0022699820631	0.0020378855086
11	0.0009939740243	-0.0013857910268	0.0004346240126	0.0009939740924
12	-0.0007993570374	-0.0007993569808	-0.0007993569808	-0.0007993569808
13	0.0014423664665	0.0014423664985	0.0014423664985	0.0014423664985
14	0.0076879210010	0.0010679134421	0.0060348076492	0.0076879209172
15	0.0096814503319	0.0147728546074	0.0109485921773	0.0096814503566
16	0.0006243090343	-0.0002988190093	0.0003992814096	0.0006243090300
17	0.0019679968418	0.0019679968999	0.0019679968999	0.0019679968999
18	0.0112963750474	0.0178629024422	0.0129308755610	0.0112963749475
19	0.0033145333224	0.0035363861409	0.0033679421796	0.0033145333487
20	0.0081629602733	0.0081629602689	0.0081629602689	0.0081629602689
21	0.0053768811587	0.0048856770630	0.0048856770630	0.0054334777313
22	0.0082119461903	0.0164610363457	0.0164610363457	0.0085451257190
23	0.0008831803228	0.0009258895976	0.0009258895976	0.0008831803223
24	0.0024257084407	0.0024257084277	0.0024257084277	0.0024257084277
25	0.0001249975622	0.0001249975490	0.0001249975490	0.0001249975490
26	0.0014837557170	0.0014837556803	0.0014837556803	0.0014837556803
27	0.0001078028256	0.0001078028502	0.0001078028502	0.0001078028502
28	0.0048456990303	0.0048456990222	0.0048456990222	0.0048456990222
29	0.0020869603879	0.0020869605144	0.0020869605144	0.0020869605144
30	0.0054131856952	0.0054131856440	0.0054131856440	0.0054131856440
31	0.0042118284970	0.0042118284890	0.0042118284890	0.0042118284890
32	0.0041601857695	-0.0069449100658	-0.0069449100658	0.0045832139416
33	0.0023082706519	0.0023082706807	0.0023082706807	0.0023082706807
34	0.0038330429937	0.0038330430827	0.0038330430827	0.0038330430827
35	0.0010768352581	0.0010768352400	0.0010768352400	0.0010768352400
36	-0.0036218169099	-0.0190465144216	-0.0190471036206	-0.0034713449209
37	0.0017923098868	0.0017923098681	0.0017923098681	0.0017923098681
38	0.0011064075235	0.0011064075085	0.0011064075085	0.0011064075085
39	0.0054232673628	0.0054232674041	0.0054232674041	0.0054232674041
40	0.0013933773478	0.0013933773538	0.0013933773538	0.0013933773538

Appendix E: Calculated delta for different fluid saturations

Blocks	delta_measured	delta_gas	delta_oil	delta_wet
1	-0.0016457174272	-0.0016457174139	-0.0016457174142	-0.0016457174142
2	-0.0010387142058	-0.0010387142028	-0.0010387142028	-0.0010387142028
3	-0.0009479108016	-0.0009479108024	-0.0009479108024	-0.0009479108024
4	-0.0023308549482	-0.0023308549761	-0.0023308549761	-0.0023308549761
5	-0.0058606876532	-0.0058606876503	-0.0058606876503	-0.0058606876503
6	-0.0043868881827	-0.0043868881716	-0.0043868881716	-0.0043868881716
7	-0.0036232628122	-0.0036232627970	-0.0036232627970	-0.0036232627970
8	-0.0028870294339	-0.0028870293986	-0.0028870293986	-0.0028870293986
9	-0.0078364580423	-0.0085057080572	-0.0079959886997	-0.0078364579679
10	-0.0033857462726	-0.0034216586941	-0.0034634208579	-0.0033857463812
11	-0.0033083897008	-0.0055806589401	-0.0038430423903	-0.0033083896535
12	-0.0088662209198	-0.0088662208026	-0.0088662208026	-0.0088662208026
13	-0.0011535206690	-0.0011535206335	-0.0011535206335	-0.0011535206335
14	-0.0112827974758	-0.0174297082663	-0.0128225106237	-0.0112827978210
15	-0.0157863693417	-0.0160248604195	-0.0159849196340	-0.0157863696886
16	-0.0023725463335	-0.0033435931245	-0.0026093588218	-0.0023725463973
17	-0.0120389096730	-0.0120389097861	-0.0120389097861	-0.0120389097861
18	0.0046635417702	0.0104704894184	0.0060954785903	0.0046635417455
19	-0.0025299525037	-0.0023412173790	-0.0024845204857	-0.0025299525491
20	-0.0059059746318	-0.0059059746077	-0.0059059746077	-0.0059059746077
21	-0.0085493164087	-0.0089395430208	-0.0089395430208	-0.0085043460684
22	-0.0300878671115	-0.0270985587551	-0.0270985587551	-0.0297080396664
23	-0.0007698856963	-0.0007338135831	-0.0007338135831	-0.0007698857141
24	-0.0026397998891	-0.0026397998543	-0.0026397998543	-0.0026397998543
25	-0.0009764280379	-0.0009764280604	-0.0009764280604	-0.0009764280604
26	0.0008834299159	0.0008834299107	0.0008834299107	0.0008834299107
27	-0.0015081414572	-0.0015081414746	-0.0015081414746	-0.0015081414746
28	-0.0033134305537	-0.0033134304962	-0.0033134304962	-0.0033134304962
29	-0.0028771396862	-0.0028771395712	-0.0028771395712	-0.0028771395712
30	0.0029667895040	0.0029667895419	0.0029667895419	0.0029667895419
31	-0.0183725006274	-0.0183725006929	-0.0183725006929	-0.0183725006929
32	-0.0138718904277	-0.0275189512391	-0.0275189512391	-0.0133355002164
33	-0.0008380598406	-0.0008380597903	-0.0008380597903	-0.0008380597903
34	-0.0001605318626	-0.0001605317536	-0.0001605317536	-0.0001605317536
35	-0.0053267789658	-0.0053267790745	-0.0053267790745	-0.0053267790745
36	-0.0186278202801	-0.0364765776389	-0.0364774386594	-0.0183929951035
37	-0.0051110552426	-0.0051110553129	-0.0051110553129	-0.0051110553129
38	-0.0085826796264	-0.0085826795839	-0.0085826795839	-0.0085826795839
39	-0.0014098945351	-0.0014098945448	-0.0014098945448	-0.0014098945448
40	-0.0076271231382	-0.0076271231097	-0.0076271231097	-0.0076271231097

Appendix F: Calculated gamma for different fluid saturations

Blocks	gamma_measured	gamma_gas	gamma_oil	gamma_wet
1	0.0053014870808	0.0053014870594	0.0053014870592	0.0053014870592
2	0.0032517823171	0.0032517823298	0.0032517823298	0.0032517823298
3	0.0026483618068	0.0026483618062	0.0026483618062	0.0026483618062
4	0.0062047414303	0.0062047414677	0.0062047414677	0.0062047414677
5	0.0186239206401	0.0186239206162	0.0186239206162	0.0186239206162
6	0.0136904341317	0.0136904340988	0.0136904340988	0.0136904340988
7	0.0096564797036	0.0096564796980	0.0096564796980	0.0096564796980
8	0.0094552017295	0.0094552016262	0.0094552016262	0.0094552016262
9	0.0201722644949	0.0201722662299	0.0201722630142	0.0201722644134
10	0.0070584668177	0.0070585503065	0.0070584751811	0.0070584669387
11	0.0076814509132	0.0076814510624	0.0076814353380	0.0076814509298
12	0.0129433281203	0.0129433280132	0.0129433280132	0.0129433280132
13	0.0044871204593	0.0044871204527	0.0044871204527	0.0044871204527
14	0.0301265774334	0.0301266863726	0.0301265192395	0.0301265779125
15	0.0414101443483	0.0414101557449	0.0414101612060	0.0414101450286
16	0.0056678111720	0.0056678130838	0.0056678047813	0.0056678113088
17	0.0221372686846	0.0221372689641	0.0221372689641	0.0221372689641
18	0.0108790595365	0.0108790942219	0.0108790543553	0.0108790594150
19	0.0098341389783	0.0098341413148	0.0098341397784	0.0098341390950
20	0.0264435302333	0.0264435301818	0.0264435301818	0.0264435301818
21	0.0248824005769	0.0248823988721	0.0248823988721	0.0248824100937
22	0.0480839139949	0.0480838265870	0.0480838265870	0.0480839275046
23	0.0028608773944	0.0028608768154	0.0028608768154	0.0028608774251
24	0.0090407427180	0.0090407426354	0.0090407426354	0.0090407426354
25	0.0019189105742	0.0019189105896	0.0019189105896	0.0019189105896
26	0.0010730144060	0.0010730143503	0.0010730143503	0.0010730143503
27	0.0027976509968	0.0027976510679	0.0027976510679	0.0027976510679
28	0.0129812353036	0.0129812351793	0.0129812351793	0.0129812351793
29	0.0088711199198	0.0088711199428	0.0088711199428	0.0088711199428
30	0.0035195459292	0.0035195458017	0.0035195458017	0.0035195458017
31	0.0425980761583	0.0425980762510	0.0425980762510	0.0425980762510
32	0.0241085387694	0.0241085136294	0.0241085136294	0.0241085244147
33	0.0046871964987	0.0046871964626	0.0046871964626	0.0046871964626
34	0.0060011947114	0.0060011946751	0.0060011946751	0.0060011946751
35	0.0110244961482	0.0110244963185	0.0110244963185	0.0110244963185
36	0.0259326805600	0.0259326594805	0.0259326594805	0.0259326588163
37	0.0116043051057	0.0116043051964	0.0116043051964	0.0116043051964
38	0.0178554348081	0.0178554347072	0.0178554347072	0.0178554347072
39	0.0125030238982	0.0125030240080	0.0125030240080	0.0125030240080
40	0.0153662632994	0.0153662632473	0.0153662632473	0.0153662632473

Appendix G:Vertical P-wave velocity versus block number at different fluid saturations

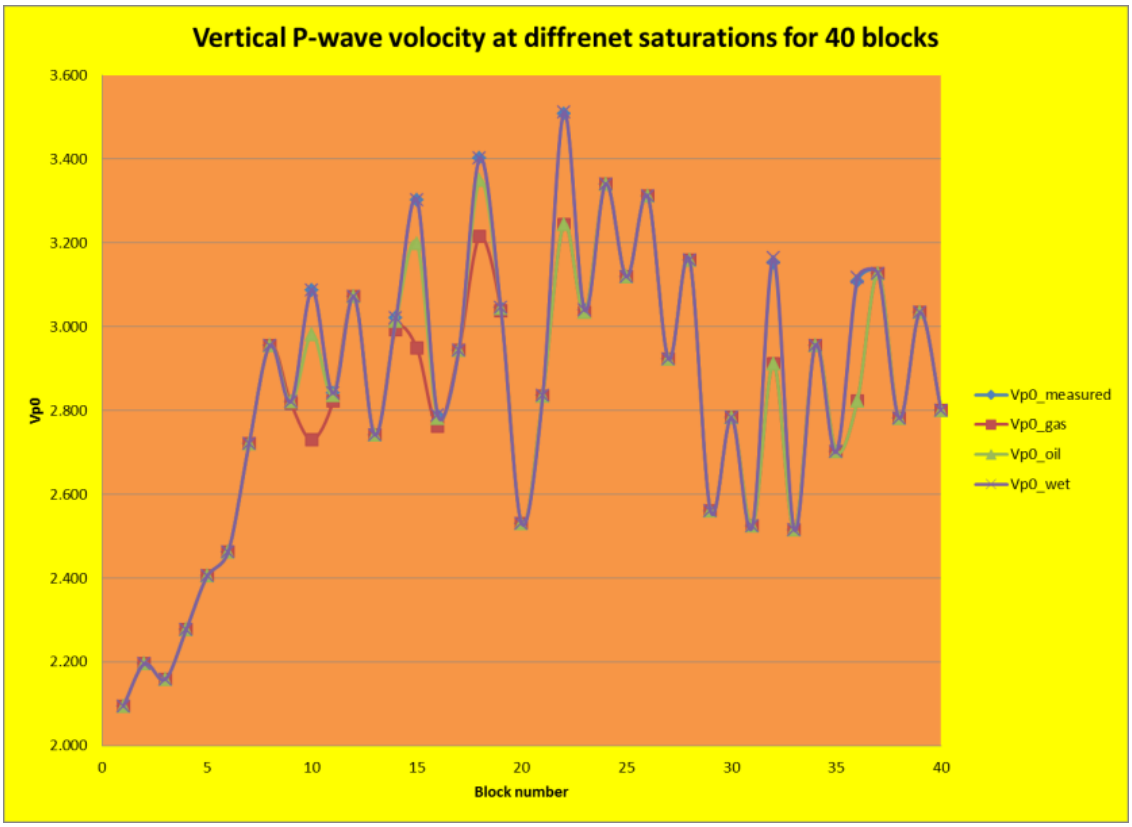

Appendix H: Vertical S-wave velocity versus block number at different fluid saturations

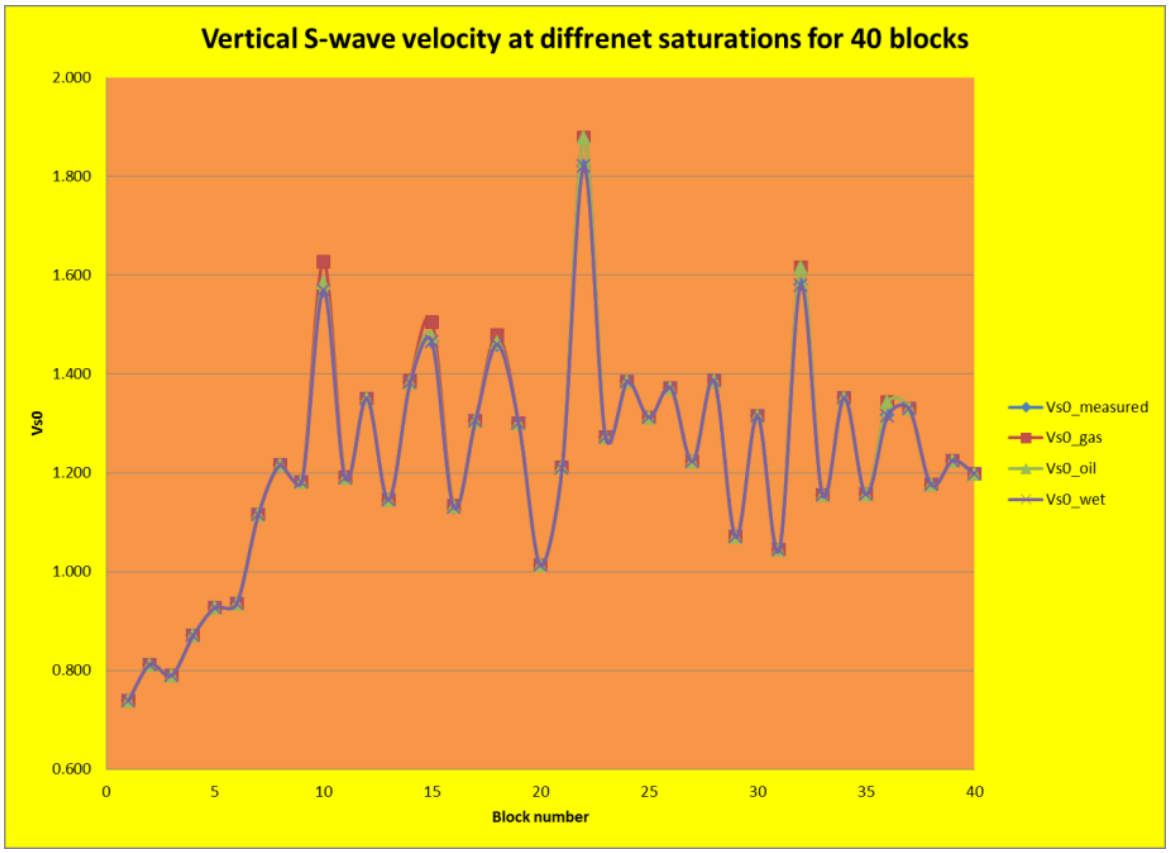

Appendix I: Gamma versus block number at different fluid saturations

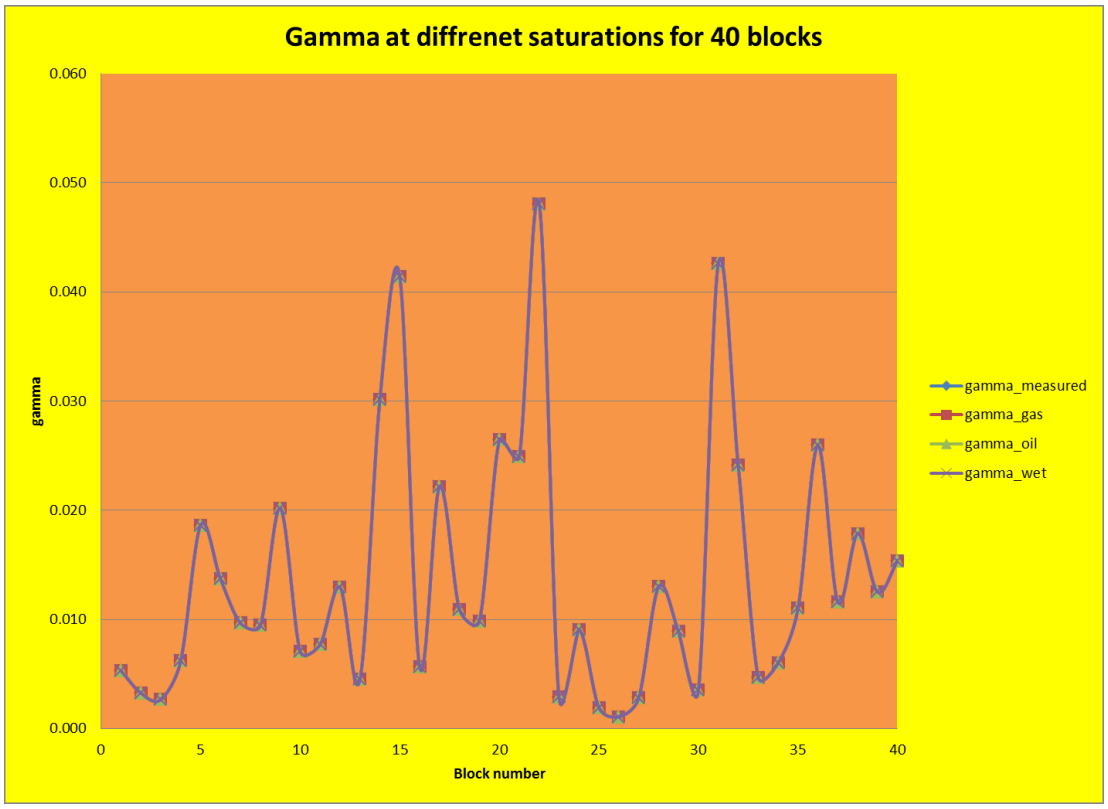

Appendix J: Epsilon versus block number at different fluid saturations

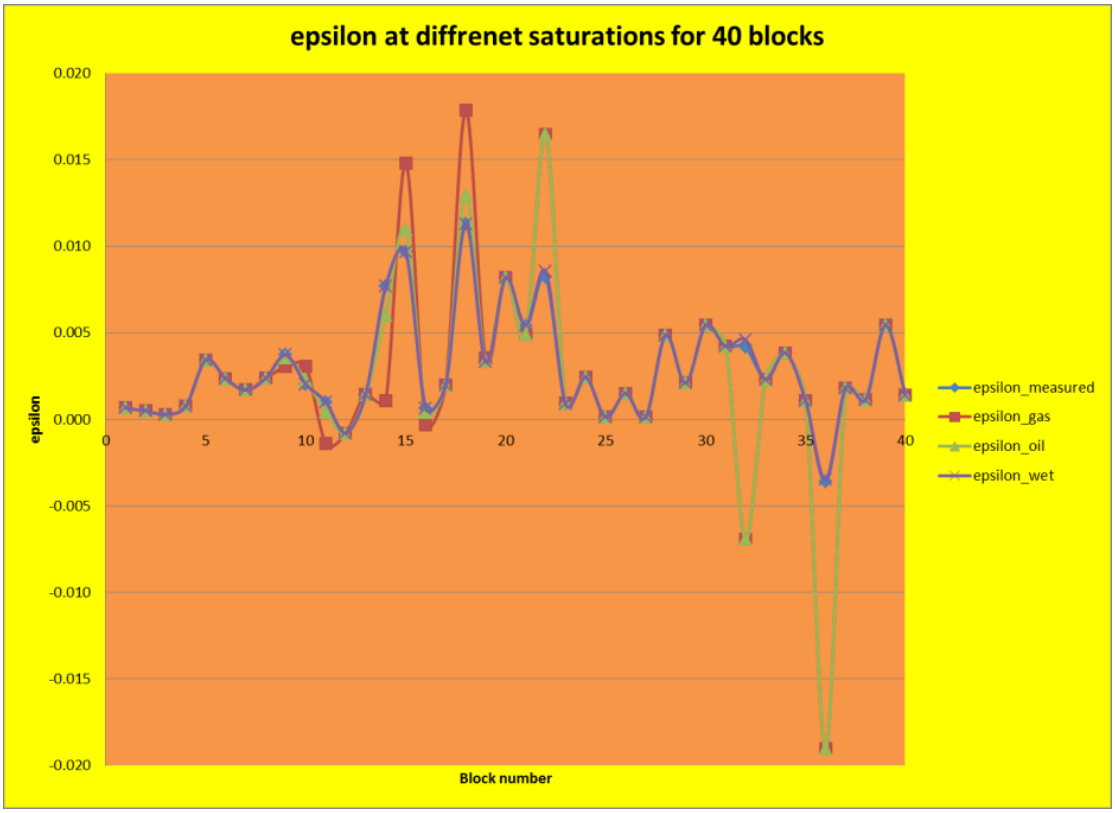

Appendix I: delta versus block number at different fluid saturations

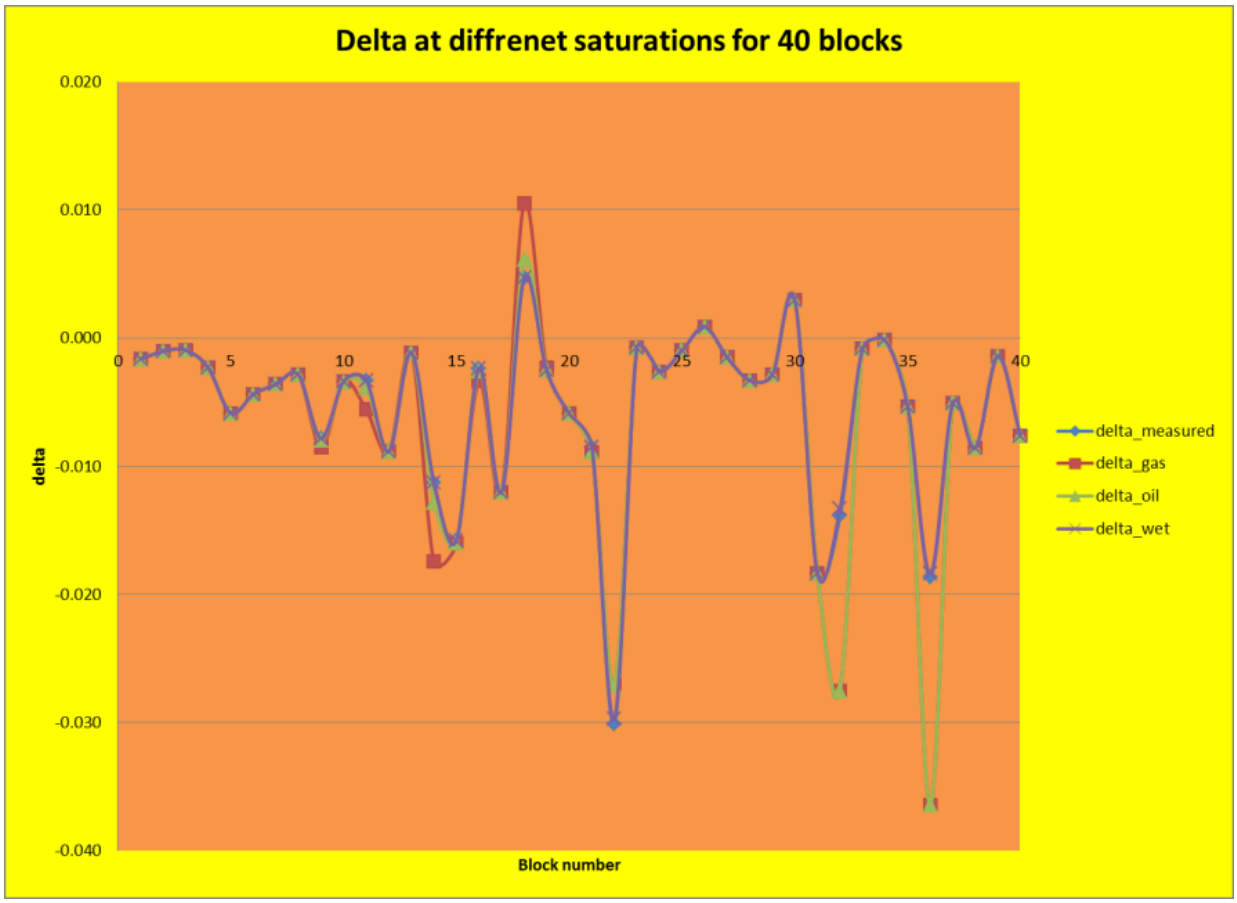

Appendix J: Matlab code

```
clear all
clc
close all
%welldata containing Vp, Vs, Rho to be used to calculate Stiffness
%coefficients for each block
mydata=xlsread('block1_wet.xlsx');
% mydata=xlsread('all_blocksgas.xlsx');
%defining column matrices with N inputs where N stands for the total number
%of thin layers to be scaled to a single layer.
N=851;
Depth=zeros(N,1);
Vp=zeros(N,1);
Vs=zeros(N,1);
Rho=zeros(N,1);
%% Asigning values to Vp,Vs, depth and rho from the imported data files
Depth=mydata(:,1);
rho=mydata(:,2);
vp=mydata(:,3);
vs=mydata(:,4);
Vp=vp/1000;
Vs=vs/1000;
%Calculating the stiffness coefficients for each layer assuming isotropic
%media
for j=1:N;
    c33(j)=(Vp(j))^2*rho(j);
    c44(j)=(Vs(j))^2*rho(j);
```

```
    c11(j)=c33(j);
    c66(j)=c44(j);
    c12(j)=c33(j)-2*c66(j);
    c13(j)=c12(j);
    A(j)=c11(j)-(((c13(j))^2)/c33(j));
    B(j)=c13(j)/c33(j);
    D(j)=(c33(j))^(-1);
    E(j)=(c44(j))^(-1);
end
%Formation of the effective homogeneous media through upscaling usung
%Backus averaging technique
    A1=mean(A);
    B1=mean(B);
    D1=mean(D);
    E1=mean(E);
    C11=A1+(B1^2*D1^(-1));
    C33=D1^(-1);
    C13=B1*D1^(-1);
    C44=E1^(-1);
    C66=mean(c66);
    Rho=mean(rho);
%calculating the effective medium velocities and anisotropic parameters
% epson, delata and gamma
Vp0=(C33/Rho)^0.5;
Vs0=(C44/Rho)^0.5;
epson=(C11-C33)/(2*C33);
delta=((C13+C44)^2-(C33-C44)^2)/((2*C33)*(C33-C44));
gamma=(C66-C44)/(2*C44);

final=[Vp0 Vs0 Rho epson delta gamma];
fprintf('%f\n', final)
xlswrite('block1',final);




%plotting results
clear all
clc
effectivemedium=xlsread('results_all.xlsx');

%loading data for normal graphs against block number
% effectivemedium=xlsread('blocks.xlsx');

% block =effectivemedium(:,1);
depth =effectivemedium(:,1);
Vp0_measured=effectivemedium(:,2);
Vp0_gas=effectivemedium(:,3);
Vp0_oil=effectivemedium(:,4);
Vp0_wet=effectivemedium(:,5);

Vs0_measured=effectivemedium(:,6);
Vs0_gas=effectivemedium(:,7);
Vs0_oil=effectivemedium(:,8);
Vs0_wet=effectivemedium(:,9);

epsilon_measured=effectivemedium(:,10);
epsilon_gas=effectivemedium(:,11);
epsilon_oil=effectivemedium(:,12);
```

```
epsilon_wet=effectivemedium(:,13);

delta_measured=effectivemedium(:,14);
delta_gas=effectivemedium(:,15);
delta_oil=effectivemedium(:,16);
delta_wet=effectivemedium(:,17);

gamma_measured=effectivemedium(:,18);
gamma_gas=effectivemedium(:,19);
gamma_oil=effectivemedium(:,20);
gamma_wet=effectivemedium(:,21);

plot(depth,epsilon_measured,'b-o')
hold on
plot(depth,epsilon_gas,'r-o')
plot(depth,epsilon_oil,'g-o')
plot(depth,epsilon_wet,'m-o')
hold off

% plot(block,Vp0_measured,'b-o')
% hold on
% plot(block,Vp0_gas,'r-o')
% plot(block,Vp0_oil,'g-o')
% plot(block,Vp0_wet,'m-o')
% hold off
```

Appendix K: Data for plotting the blocked model in excel (results_all.xls)

depth (m)	Vp0_measured	Vp0_gas	Vp0_oil	Vp0_wet	Vs0_measured	Vs0_gas	Vs0_oil	Vs0_wet	epsilon_measured	epsilon_gas	epsilon_oil	epsilon_wet	delta_measured	delta_gas	delta_oil	delta_wet	gamma_measured	gamma_gas	gamma_oil	gamma_wet
2510.4	2.094605	2.094605	2.094605	2.094605	0.738119	0.738119	0.738119	0.738119	0.00065	0.00065	0.00065	0.00065	-0.00165	-0.00165	-0.00165	-0.00165	0.005301	0.005301	0.005301	0.005301
2640	2.094605	2.094605	2.094605	2.094605	0.738119	0.738119	0.738119	0.738119	0.00065	0.00065	0.00065	0.00065	-0.00165	-0.00165	-0.00165	-0.00165	0.005301	0.005301	0.005301	0.005301
2640	2.195216	2.195215	2.195215	2.195215	0.811294	0.811294	0.811294	0.811294	0.000478	0.000478	0.000478	0.000478	-0.00104	-0.00104	-0.00104	-0.00104	0.003252	0.003252	0.003252	0.003252
2670	2.195216	2.195215	2.195215	2.195215	0.811294	0.811294	0.811294	0.811294	0.000478	0.000478	0.000478	0.000478	-0.00104	-0.00104	-0.00104	-0.00104	0.003252	0.003252	0.003252	0.003252
2670	2.158725	2.158725	2.158725	2.158725	0.790043	0.790043	0.790043	0.790043	0.000281	0.000281	0.000281	0.000281	-0.00095	-0.00095	-0.00095	-0.00095	0.002648	0.002648	0.002648	0.002648
2710	2.158725	2.158725	2.158725	2.158725	0.790043	0.790043	0.790043	0.790043	0.000281	0.000281	0.000281	0.000281	-0.00095	-0.00095	-0.00095	-0.00095	0.002648	0.002648	0.002648	0.002648
2710	2.277238	2.277238	2.277238	2.277238	0.870532	0.870532	0.870532	0.870532	0.000749	0.000749	0.000749	0.000749	-0.00233	-0.00233	-0.00233	-0.00233	0.006205	0.006205	0.006205	0.006205
2800	2.277238	2.277238	2.277238	2.277238	0.870532	0.870532	0.870532	0.870532	0.000749	0.000749	0.000749	0.000749	-0.00233	-0.00233	-0.00233	-0.00233	0.006205	0.006205	0.006205	0.006205
2800	2.404929	2.404929	2.404929	2.404929	0.926971	0.926971	0.926971	0.926971	0.003432	0.003432	0.003432	0.003432	-0.00586	-0.00586	-0.00586	-0.00586	0.018624	0.018624	0.018624	0.018624
2900	2.404929	2.404929	2.404929	2.404929	0.926971	0.926971	0.926971	0.926971	0.003432	0.003432	0.003432	0.003432	-0.00586	-0.00586	-0.00586	-0.00586	0.018624	0.018624	0.018624	0.018624
2900	2.461937	2.461937	2.461937	2.461937	0.934885	0.934885	0.934885	0.934885	0.002347	0.002347	0.002347	0.002347	-0.00439	-0.00439	-0.00439	-0.00439	0.01369	0.01369	0.01369	0.01369
2925	2.461937	2.461937	2.461937	2.461937	0.934885	0.934885	0.934885	0.934885	0.002347	0.002347	0.002347	0.002347	-0.00439	-0.00439	-0.00439	-0.00439	0.01369	0.01369	0.01369	0.01369
2925	2.721148	2.721148	2.721148	2.721148	1.115119	1.115119	1.115119	1.115119	0.001683	0.001683	0.001683	0.001683	-0.00362	-0.00362	-0.00362	-0.00362	0.009656	0.009656	0.009656	0.009656
2955	2.721148	2.721148	2.721148	2.721148	1.115119	1.115119	1.115119	1.115119	0.001683	0.001683	0.001683	0.001683	-0.00362	-0.003	-0.003	-0.0036	0.009656	0.009656	0.009656	0.009656

														62	62	2				
2955	2.955271	2.955271	2.955271	2.955271	1.215235	1.215235	1.215235	1.215235	0.002364	0.002364	0.002364	0.002364	-0.00289	-0.00289	-0.00289	-0.00289	0.009455	0.009455	0.009455	0.009455
2967	2.955271	2.955271	2.955271	2.955271	1.215235	1.215235	1.215235	1.215235	0.002364	0.002364	0.002364	0.002364	-0.00289	-0.00289	-0.00289	-0.00289	0.009455	0.009455	0.009455	0.009455
2967	2.82153	2.816042	2.820243	2.82153	1.181256	1.181702	1.181373	1.181256	0.003708	0.003042	0.00355	0.003708	-0.00784	-0.00851	-0.008	-0.00784	0.020172	0.020172	0.020172	0.020172
2979	2.82153	2.816042	2.820243	2.82153	1.181256	1.181702	1.181373	1.181256	0.003708	0.003042	0.00355	0.003708	-0.00784	-0.00851	-0.008	-0.00784	0.020172	0.020172	0.020172	0.020172
2979	3.087065	2.730262	2.981948	3.087065	1.569116	1.627745	1.583808	1.569116	0.002038	0.003065	0.00227	0.002038	-0.00339	-0.00342	-0.00346	-0.00339	0.007058	0.007059	0.007058	0.007058
2981	3.087065	2.730262	2.981948	3.087065	1.569116	1.627745	1.583808	1.569116	0.002038	0.003065	0.00227	0.002038	-0.00339	-0.00342	-0.00346	-0.00339	0.007058	0.007059	0.007058	0.007058
2981	2.84056	2.822274	2.836309	2.84056	1.189285	1.190713	1.189657	1.189285	0.000994	-0.00139	0.000435	0.000994	-0.00331	-0.00558	-0.00384	-0.00331	0.007681	0.007681	0.007681	0.007681
2985	2.84056	2.822274	2.836309	2.84056	1.189285	1.190713	1.189657	1.189285	0.000994	-0.00139	0.000435	0.000994	-0.00331	-0.00558	-0.00384	-0.00331	0.007681	0.007681	0.007681	0.007681
2985	3.071084	3.071084	3.071084	3.071084	1.349941	1.349941	1.349941	1.349941	-0.0008	-0.0008	-0.0008	-0.0008	-0.00887	-0.00887	-0.00887	-0.00887	0.012943	0.012943	0.012943	0.012943
2989	3.071084	3.071084	3.071084	3.071084	1.349941	1.349941	1.349941	1.349941	-0.0008	-0.0008	-0.0008	-0.0008	-0.00887	-0.00887	-0.00887	-0.00887	0.012943	0.012943	0.012943	0.012943
2989	2.741496	2.741496	2.741496	2.741496	1.145181	1.145181	1.145181	1.145181	0.001442	0.001442	0.001442	0.001442	-0.00115	-0.00115	-0.00115	-0.00115	0.004487	0.004487	0.004487	0.004487
2998	2.741496	2.741496	2.741496	2.741496	1.145181	1.145181	1.145181	1.145181	0.001442	0.001442	0.001442	0.001442	-0.00115	-0.00115	-0.00115	-0.00115	0.004487	0.004487	0.004487	0.004487
2998	3.020579	2.993001	3.013671	3.020579	1.382456	1.385354	1.383212	1.382456	0.007688	0.001068	0.006035	0.007688	-0.01128	-0.01743	-0.01282	-0.01128	0.030127	0.030127	0.030127	0.030127
2999	3.020579	2.993001	3.013671	3.020579	1.382456	1.385354	1.383212	1.382456	0.007688	0.001068	0.006035	0.007688	-0.01128	-0.01743	-0.01282	-0.01128	0.030127	0.030127	0.030127	0.030127
2999	3.301745	2.948902	3.197927	3.301745	1.464961	1.505576	1.475264	1.464961	0.009681	0.014773	0.010949	0.009681	-0.01579	-0.01602	-0.01598	-0.01579	0.04141	0.04141	0.04141	0.04141

3001	3.301745	2.948902	3.197927	3.301745	1.464961	1.505576	1.475264	1.464961	0.009681	0.014773	0.010949	0.009681	-0.01579	-0.01602	-0.01598	-0.01579	0.04141	0.04141	0.04141	0.04141
3001	2.788053	2.762084	2.781734	2.788053	1.130329	1.132701	1.130948	1.130329	0.000624	-0.0003	0.000399	0.000624	-0.00237	-0.00334	-0.00261	-0.00237	0.005668	0.005668	0.005668	0.005668
3003	2.788053	2.762084	2.781734	2.788053	1.130329	1.132701	1.130948	1.130329	0.000624	-0.0003	0.000399	0.000624	-0.00237	-0.00334	-0.00261	-0.00237	0.005668	0.005668	0.005668	0.005668
3003	2.943504	2.943504	2.943504	2.943504	1.304531	1.304531	1.304531	1.304531	0.001968	0.001968	0.001968	0.001968	-0.01204	-0.01204	-0.01204	-0.01204	0.022137	0.022137	0.022137	0.022137
3006	2.943504	2.943504	2.943504	2.943504	1.304531	1.304531	1.304531	1.304531	0.001968	0.001968	0.001968	0.001968	-0.01204	-0.01204	-0.01204	-0.01204	0.022137	0.022137	0.022137	0.022137
3006	3.40173	3.215239	3.350103	3.40173	1.458993	1.478605	1.464049	1.458992	0.011296	0.017863	0.012931	0.011296	0.004664	0.01047	0.006095	0.004664	0.010879	0.010879	0.010879	0.010879
3010	3.40173	3.215239	3.350103	3.40173	1.458993	1.478605	1.464049	1.458992	0.011296	0.017863	0.012931	0.011296	0.004664	0.01047	0.006095	0.004664	0.010879	0.010879	0.010879	0.010879
3010	3.045086	3.037015	3.043162	3.045086	1.299344	1.299879	1.299484	1.299344	0.003315	0.003536	0.003368	0.003315	-0.00253	-0.00234	-0.00248	-0.00253	0.009834	0.009834	0.009834	0.009834
3024	3.045086	3.037015	3.043162	3.045086	1.299344	1.299879	1.299484	1.299344	0.003315	0.003536	0.003368	0.003315	-0.00253	-0.00234	-0.00248	-0.00253	0.009834	0.009834	0.009834	0.009834
3024	2.529788	2.529788	2.529788	2.529788	1.012053	1.012052	1.012052	1.012052	0.008163	0.008163	0.008163	0.008163	-0.00591	-0.00591	-0.00591	-0.00591	0.026444	0.026444	0.026444	0.026444
3041	2.529788	2.529788	2.529788	2.529788	1.012053	1.012052	1.012052	1.012052	0.008163	0.008163	0.008163	0.008163	-0.00591	-0.00591	-0.00591	-0.00591	0.026444	0.026444	0.026444	0.026444
3041	2.835558	2.834855	2.834855	2.835635	1.2099	1.210028	1.210028	1.209883	0.005377	0.004886	0.004886	0.005433	-0.00855	-0.00894	-0.00894	-0.0085	0.024882	0.024882	0.024882	0.024882
3070.8	2.835558	2.834855	2.834855	2.835635	1.2099	1.210028	1.210028	1.209883	0.005377	0.004886	0.004886	0.005433	-0.00855	-0.00894	-0.00894	-0.0085	0.024882	0.024882	0.024882	0.024882
3070.8	3.508362	3.243188	3.243188	3.511144	1.8207	1.878367	1.878367	1.819909	0.008212	0.016461	0.016461	0.008545	-0.03009	-0.0271	-0.0271	-0.02971	0.048084	0.048084	0.048084	0.048084
3081.2	3.508362	3.243188	3.243188	3.511144	1.8207	1.878367	1.878367	1.819909	0.008212	0.016461	0.016461	0.008545	-0.03009	-0.0271	-0.0271	-0.02971	0.048084	0.048084	0.048084	0.048084
3081.2	3.039247	3.033814	3.033814	3.039247	1.272301	1.272633	1.272633	1.272301	0.000883	0.000926	0.000926	0.000883	-0.00077	-0.00073	-0.00073	-0.00077	0.002861	0.002861	0.002861	0.002861
310	3.039247	3.033	3.033	3.039	1.272301	1.272	1.272	1.272	0.000883	0.00092	0.0009	0.00088	-0.00077	-	-	-	0.002861	0.00286	0.0028	0.00286

0		814	814	247		633	633	301		6	26	3		0.00073	0.00073	0.00077		1	61	1
3100	3.340233	3.340233	3.340233	3.340233	1.384475	1.384475	1.384475	1.384475	0.002426	0.002426	0.002426	0.002426	-0.00264	-0.00264	-0.00264	-0.00264	0.009041	0.009041	0.009041	0.009041
3117	3.340233	3.340233	3.340233	3.340233	1.384475	1.384475	1.384475	1.384475	0.002426	0.002426	0.002426	0.002426	-0.00264	-0.00264	-0.00264	-0.00264	0.009041	0.009041	0.009041	0.009041
3117	3.118818	3.118818	3.118818	3.118818	1.312127	1.312127	1.312127	1.312127	0.000125	0.000125	0.000125	0.000125	-0.00098	-0.00098	-0.00098	-0.00098	0.001919	0.001919	0.001919	0.001919
3121	3.118818	3.118818	3.118818	3.118818	1.312127	1.312127	1.312127	1.312127	0.000125	0.000125	0.000125	0.000125	-0.00098	-0.00098	-0.00098	-0.00098	0.001919	0.001919	0.001919	0.001919
3121	3.311602	3.311602	3.311602	3.311602	1.371588	1.371588	1.371588	1.371588	0.001484	0.001484	0.001484	0.001484	0.000883	0.000883	0.000883	0.000883	0.001073	0.001073	0.001073	0.001073
3126	3.311602	3.311602	3.311602	3.311602	1.371588	1.371588	1.371588	1.371588	0.001484	0.001484	0.001484	0.001484	0.000883	0.000883	0.000883	0.000883	0.001073	0.001073	0.001073	0.001073
3126	2.922841	2.922841	2.922841	2.922841	1.22288	1.222888	1.222888	1.222888	0.000108	0.000108	0.000108	0.000108	-0.00151	-0.00151	-0.00151	-0.00151	0.002798	0.002798	0.002798	0.002798
3135	2.922841	2.922841	2.922841	2.922841	1.22288	1.222888	1.222888	1.222888	0.000108	0.000108	0.000108	0.000108	-0.00151	-0.00151	-0.00151	-0.00151	0.002798	0.002798	0.002798	0.002798
3135	3.159343	3.159343	3.159343	3.159343	1.385221	1.385221	1.385221	1.385221	0.004846	0.004846	0.004846	0.004846	-0.00331	-0.00331	-0.00331	-0.00331	0.012981	0.012981	0.012981	0.012981
3139	3.159343	3.159343	3.159343	3.159343	1.385221	1.385221	1.385221	1.385221	0.004846	0.004846	0.004846	0.004846	-0.00331	-0.00331	-0.00331	-0.00331	0.012981	0.012981	0.012981	0.012981
3139	2.56038	2.56038	2.56038	2.56038	1.070271	1.070271	1.070271	1.070271	0.002087	0.002087	0.002087	0.002087	-0.00288	-0.00288	-0.00288	-0.00288	0.008871	0.008871	0.008871	0.008871
3141.5	2.56038	2.56038	2.56038	2.56038	1.070271	1.070271	1.070271	1.070271	0.002087	0.002087	0.002087	0.002087	-0.00288	-0.00288	-0.00288	-0.00288	0.008871	0.008871	0.008871	0.008871
3141.5	2.782107	2.782107	2.782107	2.782107	1.314505	1.314505	1.314505	1.314505	0.005413	0.005413	0.005413	0.005413	0.002967	0.002967	0.002967	0.002967	0.00352	0.00352	0.00352	0.00352
3143	2.782107	2.782107	2.782107	2.782107	1.314505	1.314505	1.314505	1.314505	0.005413	0.005413	0.005413	0.005413	0.002967	0.002967	0.002967	0.002967	0.00352	0.00352	0.00352	0.00352
3143	2.523768	2.523767	2.523767	2.523767	1.043229	1.043229	1.043229	1.043229	0.004212	0.004212	0.004212	0.004212	-0.01837	-0.01837	-0.01837	-0.01837	0.042598	0.042598	0.042598	0.042598
3146	2.523768	2.523767	2.523767	2.523767	1.043229	1.043229	1.043229	1.043229	0.004212	0.004212	0.004212	0.004212	-0.01837	-0.01837	-0.01837	-0.01837	0.042598	0.042598	0.042598	0.042598

3146	3.153462	2.911188	2.911188	3.164372	1.580746	1.615739	1.615739	1.579152	0.00416	-0.00694	-0.00694	0.004583	-0.01387	-0.02752	-0.02752	-0.01334	0.024109	0.024109	0.024109	0.024109
3148.5	3.153462	2.911188	2.911188	3.164372	1.580746	1.615739	1.615739	1.579152	0.00416	-0.00694	-0.00694	0.004583	-0.01387	-0.02752	-0.02752	-0.01334	0.024109	0.024109	0.024109	0.024109
3148.5	2.515003	2.515003	2.515003	2.515003	1.15459	1.154559	1.154559	1.154559	0.002308	0.002308	0.002308	0.002308	-0.00084	-0.00084	-0.00084	-0.00084	0.004687	0.004687	0.004687	0.004687
3150	2.515003	2.515003	2.515003	2.515003	1.15459	1.154559	1.154559	1.154559	0.002308	0.002308	0.002308	0.002308	-0.00084	-0.00084	-0.00084	-0.00084	0.004687	0.004687	0.004687	0.004687
3150	2.955646	2.955646	2.955646	2.955646	1.350952	1.350952	1.350952	1.350952	0.003833	0.003833	0.003833	0.003833	-0.00016	-0.00016	-0.00016	-0.00016	0.006001	0.006001	0.006001	0.006001
3152	2.955646	2.955646	2.955646	2.955646	1.350952	1.350952	1.350952	1.350952	0.003833	0.003833	0.003833	0.003833	-0.00016	-0.00016	-0.00016	-0.00016	0.006001	0.006001	0.006001	0.006001
3152	2.700894	2.700894	2.700894	2.700894	1.156039	1.156039	1.156039	1.156039	0.001077	0.001077	0.001077	0.001077	-0.00533	-0.00533	-0.00533	-0.00533	0.011024	0.011024	0.011024	0.011024
3156	2.700894	2.700894	2.700894	2.700894	1.156039	1.156039	1.156039	1.156039	0.001077	0.001077	0.001077	0.001077	-0.00533	-0.00533	-0.00533	-0.00533	0.011024	0.011024	0.011024	0.011024
3156	3.108047	2.822848	2.822848	3.116215	1.31654	1.342134	1.34215	1.315462	-0.00362	-0.01905	-0.01905	-0.00347	-0.01863	-0.03648	-0.03648	-0.01839	0.025933	0.025933	0.025933	0.025933
3158	3.108047	2.822848	2.822848	3.116215	1.31654	1.342134	1.34215	1.315462	-0.00362	-0.01905	-0.01905	-0.00347	-0.01863	-0.03648	-0.03648	-0.01839	0.025933	0.025933	0.025933	0.025933
3158	3.126271	3.12627	3.12627	3.12627	1.329032	1.329032	1.329032	1.329032	0.001792	0.001792	0.001792	0.001792	-0.00511	-0.00511	-0.00511	-0.00511	0.011604	0.011604	0.011604	0.011604
3162	3.126271	3.12627	3.12627	3.12627	1.329032	1.329032	1.329032	1.329032	0.001792	0.001792	0.001792	0.001792	-0.00511	-0.00511	-0.00511	-0.00511	0.011604	0.011604	0.011604	0.011604
3162	2.781916	2.781916	2.781916	2.781916	1.176025	1.176025	1.176025	1.176025	0.001106	0.001106	0.001106	0.001106	-0.00858	-0.00858	-0.00858	-0.00858	0.017855	0.017855	0.017855	0.017855
3170	2.781916	2.781916	2.781916	2.781916	1.176025	1.176025	1.176025	1.176025	0.001106	0.001106	0.001106	0.001106	-0.00858	-0.00858	-0.00858	-0.00858	0.017855	0.017855	0.017855	0.017855
3170	3.033369	3.033369	3.033369	3.033369	1.224557	1.224557	1.224557	1.224557	0.005423	0.005423	0.005423	0.005423	-0.00141	-0.00141	-0.00141	-0.00141	0.012503	0.012503	0.012503	0.012503
3176	3.033369	3.033369	3.033369	3.033369	1.224557	1.224557	1.224557	1.224557	0.005423	0.005423	0.005423	0.005423	-0.00141	-0.001	-0.001	-0.0014	0.012503	0.012503	0.012503	0.012503

3176	2.800714	2.800714	2.800714	2.800714	1.198057	1.198057	1.198057	1.198057	0.001393	0.001393	0.001393	0.001393	-0.00763	-0.00763	-0.00763	1	0.015366	0.015366	0.015366	0.015366
3200	2.800714	2.800714	2.800714	2.800714	1.198057	1.198057	1.198057	1.198057	0.001393	0.001393	0.001393	0.001393	-0.00763	-0.00763	-0.00763	1	0.015366	0.015366	0.015366	0.015366